RESEARCH REPORT

VTT-R-04681-18 | 9.10.2018

Nuclear data uncertainty propagation to Serpent generated group and time constants

Authors: Ville Valtavirta

Confidentiality: Public

Report's title
Nuclear data uncertainty propagation to Serpent generated group and time constants

Customer, contact person, address	**Order reference**
Valtion ydinjätehuoltorahasto	SAFIR 2018
Project name	**Project number/Short name**
USVA 2018 / SAFIR 2018	117290, USVA

Summary

One application for the recently implemented collision-history based sensitivity calculation capabilities of Serpent is the propagation of nuclear data (cross section) uncertainties to the results of Serpent. Of special interest are the nuclear data related uncertainties of the group and time constants generated by Serpent.

In this work, a number of group and time constants that can be generated by Serpent are examined to identify how the sensitivity calculation capabilities could be used or extended to calculate the sensitivities that are needed to apply the Sandwich rule of deterministic first-order uncertainty propagation.

For some group and time constants the required sensitivities could be calculated either directly with the existing implementation or with small additional changes that were implemented into Serpent in this work. For other group and time constants that require additional work, the required implementations were identified and listed.

Serpent was also extended to read in multi-group covariance (nuclear data uncertainty) libraries and calculate the nuclear data uncertainties of any sensitivity responses internally during the simulation so that the nuclear data uncertainty for these responses can be output to be analyzed by the user. The output allows users to identify the total nuclear data uncertainty of a specific response as well as the contributions from the covariances (uncertainties) in the nuclear data of different reaction modes of different nuclides.

Several smaller features were also implemented to pave the way for automating the uncertainty propagation whenever group and time constants are generated by the code.

While some results of the new capabilities were compared to previous results obtained with CASMO-4E using an older covariance data library, in the future a sampling based uncertainty propagation methodology needs to be applied for the verification of the implemented routines.

Espoo, 9.10.2018

Written by	**Reviewed by**	**Accepted by**
Ville Valtavirta, Research scientist	Jaakko Leppänen, Research professor	Petri Kotiluoto, Research team leader

VTT's contact address
P.O. Box 1000, FI-02044 VTT, Finland

Distribution (customer and VTT)
SAFIR 2018 TR3

Contents

1. Introduction

One of the main applications of Serpent [1] is the generation of homogenized group and time constants for reactor simulator codes. In the recent years the application of Serpent to such tasks has become more routine [2, 3, 4]. The generation of homogenized group and time constants is a process that uses pre-processed (e.g. with NJOY) evaluated nuclear data as an input for a transport code to produce a multitude of constants describing neutron interaction in a specific target system. As the evaluated nuclear data used as input in the process is obtained through a combination of experimental and theoretical work it contains uncertainties. While some of the uncertainties in the evaluated nuclear data are still unknown, the evaluation of these uncertainties and their listing as evaluated nuclear covariance data is ongoing.

If one can assess the sensitivity of some quantities of interest (such as group constants) to perturbations in nuclear data, one can propagate the uncertainty from the available nuclear covariance data evaluations to the quantities of interest. Such sensitivity calculation capabilities were implemented to Serpent 2.1.29 in 2017 [5] based on previous work by M. Aufiero [6].

An obvious application for this capability is to combine the evaluated nuclear data uncertainties (covariances) with calculated sensitivities of any generated group constants to perturbations in nuclear data in order to obtain the nuclear data related uncertainty of the generated group constants. The name of this process is uncertainty propagation.

This report describes the extension of Serpent to combine the sensitivity calculation capabilities with evaluated covariance data resulting in estimates of nuclear data uncertainty for various output quantities, most notably in group and time constants. A large part of such an extension is related to the ability of Serpent to read in, process and interact with the nuclear covariance data. The remaining part handles the calculation of the sensitivities of the different group and time constants to nuclear data perturbation, a process that needs to be tailored in an individual manner for many of the generated group and time constants.

The approach for this project was as follows:

1. Extend Serpent to read in, process and utilize nuclear covariance data from a relevant source.
2. Extend Serpent to combine the covariance data with calculated sensitivities to produce output uncertainties during runtime.
3. Formulate the theoretical and practical approach of calculating sensitivities for the different group and time constants.
4. Implement the calculation of the sensitivities and the propagation of uncertainties for those group and time constants that do not require extensive modifications to the code.

The implementation of the sensitivity calculation for certain group/time constants as well as the automatic set up of the uncertainty propagation whenever group constants are being generated with covariance data are left as future work. Implementing the calculation of the remaining sensitivity coefficients should be straightforward as the required steps are described in this report.

2. Background

This section describes the background information on sensitivities (Sec. 2.1), deterministic uncertainty propagation (Sec. 2.2) and the calculation of sensitivities with Serpent (Sec. 2.3) that a reader might need to understand the later sections.

2.1 Theoretical background on sensitivities

In this report the term "sensitivity coefficient" (or simply "sensitivity") will be used to refer to the relative change in a response R due to a relative change in a perturbed quantity P and will be denoted with

$$S_P^R = \frac{\frac{\mathrm{d}R}{R}}{\frac{\mathrm{d}P}{P}} = \frac{P}{R}\frac{\mathrm{d}R}{\mathrm{d}P} \tag{1}$$

In the following, a few helpful relations are derived to be used later in the report.

Sensitivity of an inverse of a response:

$$S_P^{\frac{1}{R}} = \frac{\frac{\mathrm{d}R^{-1}}{R^{-1}}}{\frac{\mathrm{d}P}{P}} = RP\frac{\mathrm{d}R^{-1}}{\mathrm{d}P} = RP(-R^{-2})\frac{\mathrm{d}R}{\mathrm{d}P} = -\frac{P}{R}\frac{\mathrm{d}R}{\mathrm{d}P} = -S_P^R \tag{2}$$

Sensitivity of a product (A and B are two separate responses):

$$\begin{aligned} S_P^{AB} &= \frac{\frac{\mathrm{d}AB}{AB}}{\frac{\mathrm{d}P}{P}} = \frac{P}{AB}\frac{\mathrm{d}}{\mathrm{d}P}AB = \frac{P}{AB}\left(B\frac{\mathrm{d}A}{\mathrm{d}P} + A\frac{\mathrm{d}B}{\mathrm{d}P}\right) \\ &= \frac{P}{A}\frac{\mathrm{d}A}{\mathrm{d}P} + \frac{P}{B}\frac{\mathrm{d}B}{\mathrm{d}P} = S_P^A + S_P^B \end{aligned} \tag{3}$$

Sensitivity of a ratio (could also be obtained from the two previous derivations):

$$\begin{aligned} S_P^{A/B} &= \frac{\frac{\mathrm{d}A/B}{A/B}}{\frac{\mathrm{d}P}{P}} = \frac{BP}{A}\frac{\mathrm{d}}{\mathrm{d}P}\frac{A}{B} = \frac{BP}{A}\left(\frac{1}{B}\frac{\mathrm{d}A}{\mathrm{d}P} - \frac{A}{B^2}\frac{\mathrm{d}B}{\mathrm{d}P}\right) \\ &= \frac{P}{A}\frac{\mathrm{d}A}{\mathrm{d}P} - \frac{P}{B}\frac{\mathrm{d}B}{\mathrm{d}P} = S_P^A - S_P^B \end{aligned} \tag{4}$$

In a (perhaps) interesting manner, the sensitivities of sums or differences of responses have slightly more complex forms depending also on the magnitude of the responses. Sum:

$$\begin{aligned} S_P^{A+B} &= \frac{\frac{\mathrm{d}(A+B)}{(A+B)}}{\frac{\mathrm{d}P}{P}} = \frac{P}{A+B}\frac{\mathrm{d}}{\mathrm{d}P}(A+B) = \frac{P}{A+B}\left(\frac{\mathrm{d}A}{\mathrm{d}P} + \frac{\mathrm{d}B}{\mathrm{d}P}\right) \\ &= \frac{1}{A+B}\left(A\frac{P}{A}\frac{\mathrm{d}A}{\mathrm{d}P} + B\frac{P}{B}\frac{\mathrm{d}B}{\mathrm{d}P}\right) \\ &= \frac{A}{A+B}S_P^A + \frac{B}{A+B}S_P^B \end{aligned} \tag{5}$$

Similarly, the difference will yield

$$
\begin{aligned}
S_P^{A-B} &= \frac{\frac{\mathrm{d}(A-B)}{(A-B)}}{\frac{\mathrm{d}P}{P}} = \frac{P}{A-B}\frac{\mathrm{d}}{\mathrm{d}P}(A-B) = \frac{P}{A-B}\left(\frac{\mathrm{d}A}{\mathrm{d}P} - \frac{\mathrm{d}B}{\mathrm{d}P}\right) \\
&= \frac{1}{A-B}\left(A\frac{P}{A}\frac{\mathrm{d}A}{\mathrm{d}P} - B\frac{P}{B}\frac{\mathrm{d}B}{\mathrm{d}P}\right) \\
&= \frac{A}{A-B}S_P^A - \frac{B}{A-B}S_P^B
\end{aligned} \tag{6}
$$

Finally, it should be noted that the sensitivity of a response R multiplied by a constant α is simply

$$
S_P^{\alpha R} = \frac{\frac{\mathrm{d}(\alpha R)}{(\alpha R)}}{\frac{\mathrm{d}P}{P}} = \frac{P}{\alpha R}\frac{\mathrm{d}}{\mathrm{d}P}(\alpha R) = \frac{P}{\alpha R}\alpha\frac{\mathrm{d}}{\mathrm{d}P}R = \frac{P}{R}\frac{\mathrm{d}R}{\mathrm{d}P} = S_P^R. \tag{7}
$$

2.2 Deterministic uncertainty propagation

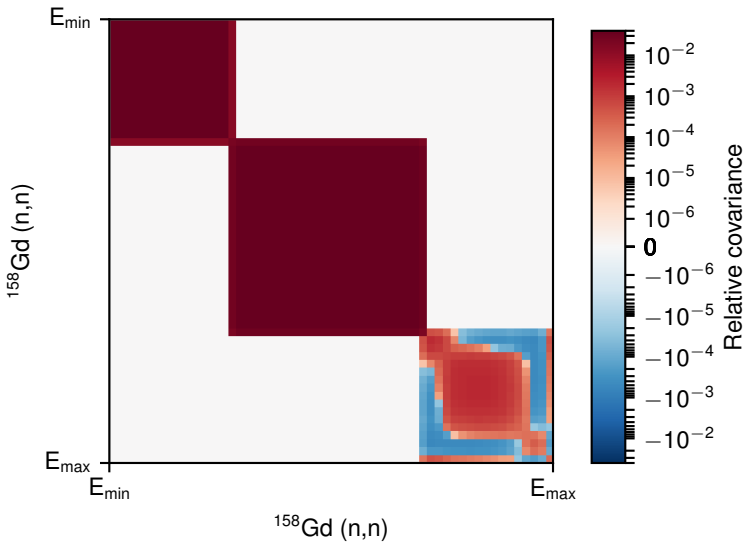

Figure 1. 56 group relative covariance of the elastic scattering cross section of ^{158}Gd. *(scale.rev08.56groupcov7.1)*

The nuclear data covariances are usually processed into a multi-group format as in the relative covariance of ^{158}Gd elastic scattering cross section shown in Fig. 1. If we know the sensitivity of a response R to the perturbation of the cross section X in each of the energy groups we can use the first-order uncertainty propagation formula (Sandwich rule) to collapse the covariance data with the sensitivities

$$
\mathrm{Cov}_X^R \approx (\overline{\mathbf{S}}_X^R)^T \overline{\overline{\mathrm{Cov}}}_{X,X} \overline{\mathbf{S}}_X^R, \tag{8}
$$

where $\overline{\mathbf{S}}_X^R \in \mathbb{R}^{N_g \times 1}$ is the sensitivity vector containing the group sensitivities, $\overline{\overline{\mathrm{Cov}}}_{X,X} \in \mathbb{R}^{N_g \times N_g}$ is the covariance matrix containing the group covariances and N_g is the number of energy

groups. The propagated nuclear data uncertainty for response R can then be obtained as the square root of the covariance:

$$\mathrm{Unc}_X^R = \sqrt{\mathrm{Cov}_X^R}. \tag{9}$$

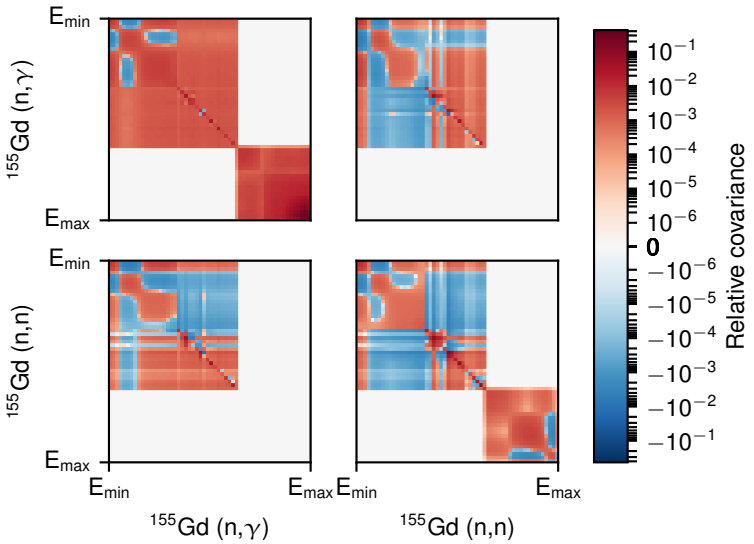

Figure 2. 56 group relative covariances of the elastic scattering and radiative capture cross sections of ^{155}Gd*. (scale.rev08.56groupcov7.1)*

Often, the data for a specific cross section has covariances not simply against itself but against some other reaction modes of the same nuclide or even some reaction modes of different nuclides. Figure 2 shows an example of such covariances between the elastic scattering and radiative capture cross sections of ^{155}Gd. In such a case, the Sandwich rule can be applied using the whole block matrix containing all four of the single-reaction covariance data (capture-capture, capture-elastic, elastic-capture and elastic-elastic) as the covariance matrix and including sensitivities of both reaction modes to the sensitivity vector:

$$\mathrm{Cov}_{2+102}^R \approx \begin{bmatrix} (\bar{\mathbf{S}}_{102}^R)^T & (\bar{\mathbf{S}}_2^R)^T \end{bmatrix} \begin{bmatrix} \overline{\overline{\mathrm{Cov}}}_{102,102} & \overline{\overline{\mathrm{Cov}}}_{102,2} \\ \overline{\overline{\mathrm{Cov}}}_{2,102} & \overline{\overline{\mathrm{Cov}}}_{2,2} \end{bmatrix} \begin{bmatrix} \bar{\mathbf{S}}_{102}^R \\ \bar{\mathbf{S}}_2^R \end{bmatrix} \tag{10}$$

Here the lower indices refer to the reaction mode MT-number (2 is elastic scattering, 102 is radiative capture) and the block matrix of covariance matrices refers to the block matrix shown in Fig. 2. The downside of this approach is the fact that the covariance of the response R coming from the different reaction covariances (2,2), (102,102) and (2,102) get lumped up to the same resulting covariance and cannot be examined separately.

For the separation of the different sources of covariance (uncertainty) we can work Eq. 10 into a form where the different contributions are separated:

$$\mathrm{Cov}^R_{2+102} \approx \begin{bmatrix} (\bar{\mathbf{S}}^R_{102})^T & (\bar{\mathbf{S}}^R_2)^T \end{bmatrix} \begin{bmatrix} \overline{\overline{\mathrm{Cov}}}_{102,102} & \overline{\overline{\mathrm{Cov}}}_{102,2} \\ \overline{\overline{\mathrm{Cov}}}_{2,102} & \overline{\overline{\mathrm{Cov}}}_{2,2} \end{bmatrix} \begin{bmatrix} \bar{\mathbf{S}}^R_{102} \\ \bar{\mathbf{S}}^R_2 \end{bmatrix}$$

$$\mathrm{Cov}^R_{2+102} \approx \begin{bmatrix} (\bar{\mathbf{S}}^R_{102})^T & (\bar{\mathbf{S}}^R_2)^T \end{bmatrix} \begin{bmatrix} \overline{\overline{\mathrm{Cov}}}_{102,102}\bar{\mathbf{S}}^R_{102} + \overline{\overline{\mathrm{Cov}}}_{102,2}\bar{\mathbf{S}}^R_2 \\ \overline{\overline{\mathrm{Cov}}}_{2,102}\bar{\mathbf{S}}^R_{102} + \overline{\overline{\mathrm{Cov}}}_{2,2}\bar{\mathbf{S}}^R_2 \end{bmatrix}$$

$$\mathrm{Cov}^R_{2+102} \approx (\bar{\mathbf{S}}^R_{102})^T\overline{\overline{\mathrm{Cov}}}_{102,102}\bar{\mathbf{S}}^R_{102} + (\bar{\mathbf{S}}^R_{102})^T\overline{\overline{\mathrm{Cov}}}_{102,2}\bar{\mathbf{S}}^R_2 + (\bar{\mathbf{S}}^R_2)^T\overline{\overline{\mathrm{Cov}}}_{2,102}\bar{\mathbf{S}}^R_{102} + (\bar{\mathbf{S}}^R_2)^T\overline{\overline{\mathrm{Cov}}}_{2,2}\bar{\mathbf{S}}^R_2$$

$$\mathrm{Cov}^R_{2+102} \approx (\bar{\mathbf{S}}^R_{102})^T\overline{\overline{\mathrm{Cov}}}_{102,102}\bar{\mathbf{S}}^R_{102} + \begin{bmatrix} (\bar{\mathbf{S}}^R_{102})^T & (\bar{\mathbf{S}}^R_2)^T \end{bmatrix} \begin{bmatrix} 0 & \overline{\overline{\mathrm{Cov}}}_{102,2} \\ \overline{\overline{\mathrm{Cov}}}_{2,102} & 0 \end{bmatrix} \begin{bmatrix} \bar{\mathbf{S}}^R_{102} \\ \bar{\mathbf{S}}^R_2 \end{bmatrix} + (\bar{\mathbf{S}}^R_2)^T\overline{\overline{\mathrm{Cov}}}_{2,2}\bar{\mathbf{S}}^R_2$$

$$\mathrm{Cov}^R_{2+102} \approx \mathrm{Cov}^R_{102} + \mathrm{Cov}^R_{(2,102)} + \mathrm{Cov}^R_2$$

Basically, we can separate the effects of the self-covariances of MT 2 and MT 102 from the cross-covariance between the two. This requires us to process the block covariance matrix in Fig. 2 into the three different matrices shown in Fig. 3:

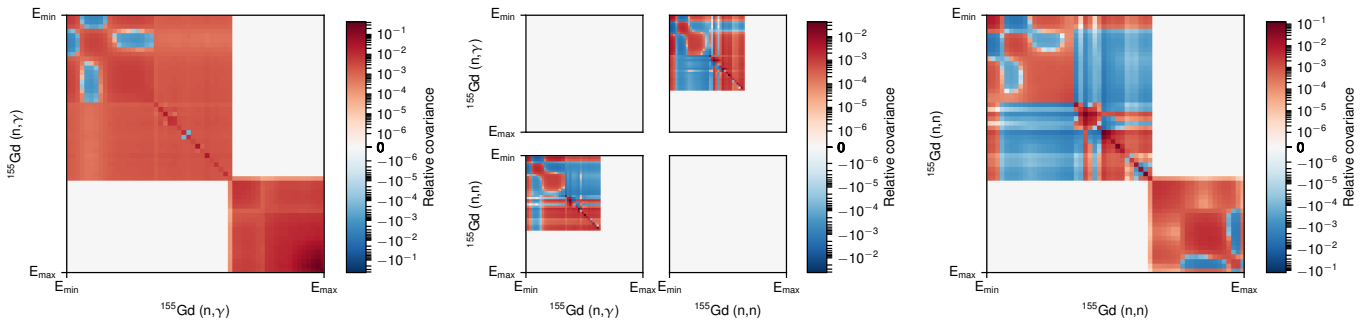

Figure 3. The covariances from the block matrix shown in Fig. 2 separated into three separate matrices, each containing either a self-covariance of a single reaction mode or a cross-covariance of two different reaction modes.

By separating the different reaction modes from the block matrices, we can separate the different sources of variance (and uncertainty) coming from the different reaction modes. While the covariance data can be read from processed covariance data files, the sensitivity vectors need to be calculated with Serpent.

2.3 Calculating sensitivities with Serpent

The sensitivity calculation capabilities of Serpent are based on a collision-history approach [6] with the current implementation being described in a separate conference publication [5].

The methodology can be used to calculate sensitivities of various responses R to various perturbations P. The possible responses include

1. The effective multiplication factor ($R = k_{\mathrm{eff.}}$).
2. Reaction rate ratios, i.e. responses in the form of $R = \frac{\langle \Sigma_1, \phi \rangle}{\langle \Sigma_2, \phi \rangle}$.
   - With next to no additional work more general responses of the form $R = \frac{\mathrm{DET}_1}{\mathrm{DET}_2}$, i.e. the ratio of two quantities tallied with implicit or analog Serpent detectors can be used.

3. Adjoint-weighted quantities (bilinear ratios) in the form of $R = \frac{\langle \phi^\dagger, \Sigma_1 \phi \rangle}{\langle \phi^\dagger, \Sigma_2 \phi \rangle}$. These types of responses include
   (a) The effective delayed neutron fraction ($R = \beta_{\text{eff.}}$).
   (b) Prompt neutron lifetime ($R = \ell_{\text{eff.}}$).
   (c) Coolant density reactivity coefficient ($R = \alpha_{\text{cool.}}$).

For each of these responses, the sensitivity can be calculated with respect to a perturbation in the cross section of a specific reaction mode of a specific nuclide over a specific energy interval (group). This allows Serpent to calculate the energy group wise sensitivity vectors for different reaction modes of different nuclides that are required to apply the Sandwich rule (Eq. 8). One such calculated group-wise sensitivity ($\overline{\mathbf{S}}$-vector) is shown in Fig. 4.

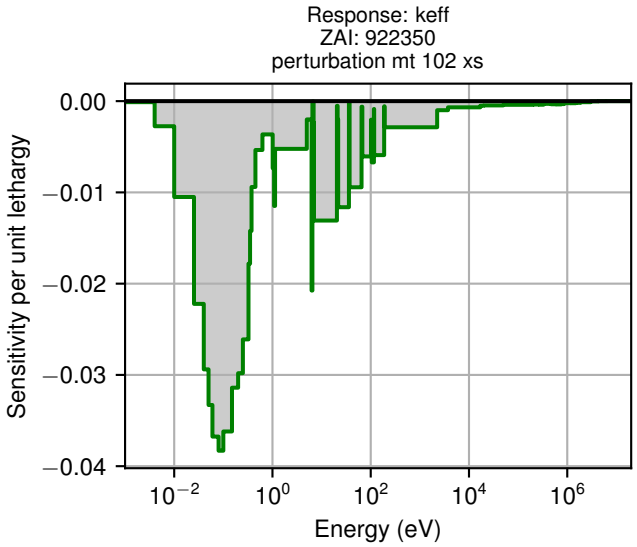

Figure 4. Sensitivity of the k_{eff} of a PWR-pin cell geometry to the capture cross section of ^{235}U calculated with Serpent. Tallied on the SCALE 56 energy group structure.

$\ell_{\text{eff.}}$ and $\beta_{\text{eff.}}$, two important time constants can be directly calculated using the sensitivity approach for the adjoint-weighted quantities and most of the group constants are of the form

$$R = \frac{\langle \Sigma_1, \phi \rangle_g}{\langle \Sigma_2, \phi \rangle_g} = \frac{\int_V \int_{E_g}^{E_{g-1}} \Sigma_1(\vec{r}, E)\phi(\vec{r}, E) \mathrm{d}E \mathrm{d}^3 r}{\int_V \int_{E_g}^{E_{g-1}} \Sigma_2(\vec{r}, E)\phi(\vec{r}, E) \mathrm{d}E \mathrm{d}^3 r} \tag{11}$$

with $\Sigma_2(\vec{r}, E) = 1$.

The first order estimate for the sensitivity of such a reaction rate ratio [6] includes direct and indirect terms:

$$S_P^R = \frac{\left\langle \frac{\partial \Sigma_1}{\partial P/P}, \phi \right\rangle_g}{\langle \Sigma_1, \phi \rangle_g} - \frac{\left\langle \frac{\partial \Sigma_2}{\partial P/P}, \phi \right\rangle_g}{\langle \Sigma_2, \phi \rangle_g} + \frac{\left\langle \Sigma_1, \frac{\partial \phi}{\partial P/P} \right\rangle_g}{\langle \Sigma_1, \phi \rangle_g} - \frac{\left\langle \Sigma_2, \frac{\partial \phi}{\partial P/P} \right\rangle_g}{\langle \Sigma_2, \phi \rangle_g}, \tag{12}$$

of which the calculation of the indirect term has been previously implemented into Serpent [5, 6].

One obvious question after noting that the sensitivities of reaction rate or detector ratios can be calculated is whether the sensitivity of a single reaction rate or a detector can be calculated, i.e. whether it is possible to use

$$R = \langle \Sigma_1, \phi \rangle$$

or

$$R = \mathrm{DET}_1.$$

In the current application, where Serpent is run in the criticality source mode this is a rather misleading question: In the criticality source mode, the normalization of the simulation is a free parameter and the detector tally values are normalized with a scalar multiplier in order to fix either the fission power, source rate or some other reaction rate to a user specified value X. This means that[1] the output of our detector 1 is actually the tallied detector value multiplied with a normalization coefficient N

$$\mathrm{DET}_1 = N \langle \Sigma_1, \phi \rangle = N\mathrm{DET}_1^0,$$

where the superscript 0 indicates the tallied value and the normalization coefficient N is chosen so that the detector tally value for another detector tallying the normalization reaction rate (e.g. fission power) will be X:

$$\mathrm{DET}_{\mathrm{norm}} = N \langle \Sigma_{\mathrm{norm}}, \phi \rangle = N\mathrm{DET}_{\mathrm{norm}}^0 = X,$$

which means that

$$N = \frac{X}{\mathrm{DET}_{\mathrm{norm}}^0}$$

and

$$\mathrm{DET}_1 = X \frac{\mathrm{DET}_1^0}{\mathrm{DET}_{\mathrm{norm}}^0}.$$

Simply put, the output values of detectors in criticality source simulations are already reaction rate ratios. The sensitivities of singular detector output values to perturbations shall thus be calculated as sensitivities of the detector ratio between the detector of interest and the normalization detector, e.g. a fission power detector covering the whole system.

[1] Not going into detail on the specific implementation.

3. Group and time constants considered in this work

We will derive methods for calculating the sensitivities for the following group and time-constants required by HEXTRAN and TRAB3D and generated by Serpent:

The two-group constants:

- **Diffusion coefficient (D).**
- **Absorption cross section (Σ_a).**
- **Fission production cross section ($\nu\Sigma_f$).**
- **Fission cross section (Σ_f).**
- **Energy per fission (κ)**
- **Inverse velocity of prompt neutrons ($1/v_p$).**
- **Discontinuity factors.**
- **Effective fission yield of fission poisons.**
- **Microscopic absorption cross sections of the fission poisons.**
- $\Sigma_{1\to 2}$ **Slowing down cross section from fast to thermal group.**

Time-constants:

- β_i **Delayed neutron fractions for each group.**
- λ_i **Delayed neutron group wise decay constants.**

Reflector constants:

- **Albedos: Total or partial.**

4. Theoretical work for calculating the required sensitivity coefficients

The problem is now to either formulate the required responses in the form of the familiar responses described in Section 2.3 for which sensitivity constants can already be calculated or to apply additional theoretical work into finding ways to calculate the sensitivities for new responses.

It should be noted that all sensitivities calculated in the manner described in the following sections will be for non-leakage corrected group constants. Propagation of the nuclear data uncertainties through the leakage correction is not considered in this report.

Serpent uses an intermediate multi-group energy group structure to tally relevant parameters and uses either direct or inverse energy group condensation to obtain the few-group constants. Eventually we may want to conduct similar condensations for the multi-group sensitivity coefficients so the derivation for such a process is presented in the following.

4.1 Direct energy group condensation

Going from multi-group (group index h) to few-group (group index g) for estimate Θ via direct energy group condensation is achieved through:

$$\Theta_g = \frac{\sum_{h\in g} \Theta_h \Phi_h}{\sum_{h\in g} \Phi_h}$$

The sensitivity of the condensed estimate (group g) can be written with the help of the multi-group estimates as:

$$S_P^{\Theta_g} = \frac{\frac{\mathrm{d}\Theta_g}{\Theta_g}}{\frac{\mathrm{d}P}{P}} = \frac{1}{\Theta_g} P \frac{\mathrm{d}\Theta_g}{\mathrm{d}P} = \frac{\sum_{h\in g} \Phi_h}{\sum_{h\in g} \Theta_h \Phi_h} P \frac{\mathrm{d}}{\mathrm{d}P} \frac{\sum_{h\in g} \Theta_h \Phi_h}{\sum_{h\in g} \Phi_h} \tag{13}$$

Expanding the derivative yields

$$S_P^{\Theta_g} = \frac{\sum_{h\in g} \Phi_h}{\sum_{h\in g} \Theta_h \Phi_h} P \left(\frac{\frac{\mathrm{d}}{\mathrm{d}P} \sum_{h\in g} \Theta_h \Phi_h}{\sum_{h\in g} \Phi_h} - \frac{\sum_{h\in g} \Theta_h \Phi_h}{\left(\sum_{h\in g} \Phi_h\right)^2} \frac{\mathrm{d}}{\mathrm{d}P} \sum_{h\in g} \Phi_h \right) \tag{14}$$

from where we can multiply the first fraction into the parentheses to obtain

$$S_P^{\Theta_g} = P \left(\frac{\frac{\mathrm{d}}{\mathrm{d}P} \sum_{h\in g} \Theta_h \Phi_h}{\sum_{h\in g} \Theta_h \Phi_h} - \frac{1}{\sum_{h\in g} \Phi_h} \frac{\mathrm{d}}{\mathrm{d}P} \sum_{h\in g} \Phi_h \right). \tag{15}$$

If we take the derivatives inside the summations, we'll have

$$S_P^{\Theta_g} = P \left(\frac{\sum_{h\in g} \left(\frac{\mathrm{d}\Theta_h}{\mathrm{d}P} \Phi_h + \Theta_h \frac{\mathrm{d}\Phi_h}{\mathrm{d}P} \right)}{\sum_{h\in g} \Theta_h \Phi_h} - \frac{1}{\sum_{h\in g} \Phi_h} \sum_{h\in g} \frac{\mathrm{d}\Phi_h}{\mathrm{d}P} \right). \tag{16}$$

Based on the definition of a sensitivity coefficient we have

$$\frac{\mathrm{d}\Theta_h}{\mathrm{d}P} = \frac{\Theta_h}{P} S_P^{\Theta_h}$$
$$\frac{\mathrm{d}\Phi_h}{\mathrm{d}P} = \frac{\Phi_h}{P} S_P^{\Phi_h},$$

which leads to

$$S_P^{\Theta_g} = P \left(\frac{\sum_{h\in g} \left(\frac{\Theta_h}{P} S_P^{\Theta_h} \Phi_h + \Theta_h \frac{\Phi_h}{P} S_P^{\Phi_h} \right)}{\sum_{h\in g} \Theta_h \Phi_h} - \frac{1}{\sum_{h\in g} \Phi_h} \sum_{h\in g} \frac{\Phi_h}{P} S_P^{\Phi_h} \right) \tag{17}$$

and finally

$$S_P^{\Theta_g} = \frac{\sum_{h\in g} \left(\Theta_h S_P^{\Theta_h} \Phi_h + \Theta_h \Phi_h S_P^{\Phi_h} \right)}{\sum_{h\in g} \Theta_h \Phi_h} - \frac{1}{\sum_{h\in g} \Phi_h} \sum_{h\in g} \Phi_h S_P^{\Phi_h} \tag{18}$$

or

$$S_P^{\Theta_g} = \frac{\sum_{h\in g} \Theta_h \Phi_h \left(S_P^{\Theta_h} + S_P^{\Phi_h} \right)}{\sum_{h\in g} \Theta_h \Phi_h} - \frac{\sum_{h\in g} \Phi_h S_P^{\Phi_h}}{\sum_{h\in g} \Phi_h}. \tag{19}$$

If Θ is a homogenized multi-group cross section, the first term is simply averaging the reaction rate using the sum of the cross section and flux sensitivities as a weighting factor. The second term is simply the average flux when the flux sensitivity is used as a weighting factor.

4.2 Inverse energy group condensation

Going from multi-group (group index *h*) to few-group (group index *g*) for estimate Θ via inverse energy group condensation is achieved through:

$$\frac{1}{\Theta_g} = \frac{\sum_{h\in g} \frac{1}{\Theta_h} \Phi_h}{\sum_{h\in g} \Phi_h} \Leftrightarrow \Theta_g = \frac{\sum_{h\in g} \Phi_h}{\sum_{h\in g} \frac{1}{\Theta_h} \Phi_h}$$

In order to somewhat follow the derivation of the direct energy group condensation we'll first derive

$$S_P^{\frac{1}{\Theta_g}}$$

and use Eq. 2 to obtain

$$S_P^{\Theta_g}.$$

We'll start with:

$$S_P^{\frac{1}{\Theta_g}} = \frac{\frac{\mathrm{d}\Theta_g^{-1}}{\Theta_g^{-1}}}{\frac{\mathrm{d}P}{P}} = \Theta_g P \frac{\mathrm{d}\Theta_g^{-1}}{\mathrm{d}P} = \frac{\sum_{h\in g} \Phi_h}{\sum_{h\in g} \frac{1}{\Theta_h} \Phi_h} P \frac{\mathrm{d}}{\mathrm{d}P} \frac{\sum_{h\in g} \frac{1}{\Theta_h} \Phi_h}{\sum_{h\in g} \Phi_h} \tag{20}$$

Expanding the derivative yields

$$S_P^{\frac{1}{\Theta_g}} = \frac{\sum_{h\in g}\Phi_h}{\sum_{h\in g}\frac{1}{\Theta_h}\Phi_h} P \left(\frac{\frac{\mathrm{d}}{\mathrm{d}P}\sum_{h\in g}\frac{1}{\Theta_h}\Phi_h}{\sum_{h\in g}\Phi_h} - \frac{\sum_{h\in g}\frac{1}{\Theta_h}\Phi_h}{\left(\sum_{h\in g}\Phi_h\right)^2}\frac{\mathrm{d}}{\mathrm{d}P}\sum_{h\in g}\Phi_h \right) \tag{21}$$

from where we can multiply the first fraction into the parentheses to obtain

$$S_P^{\frac{1}{\Theta_g}} = P \left(\frac{\frac{\mathrm{d}}{\mathrm{d}P}\sum_{h\in g}\frac{1}{\Theta_h}\Phi_h}{\sum_{h\in g}\frac{1}{\Theta_h}\Phi_h} - \frac{1}{\sum_{h\in g}\Phi_h}\frac{\mathrm{d}}{\mathrm{d}P}\sum_{h\in g}\Phi_h \right). \tag{22}$$

If we take the derivatives inside the summations, we'll have

$$S_P^{\frac{1}{\Theta_g}} = P \left(\frac{\sum_{h\in g}\left(\frac{\mathrm{d}\frac{1}{\Theta_h}}{\mathrm{d}P}\Phi_h + \frac{1}{\Theta_h}\frac{\mathrm{d}\Phi_h}{\mathrm{d}P}\right)}{\sum_{h\in g}\frac{1}{\Theta_h}\Phi_h} - \frac{1}{\sum_{h\in g}\Phi_h}\sum_{h\in g}\frac{\mathrm{d}\Phi_h}{\mathrm{d}P} \right), \tag{23}$$

which is equal to

$$S_P^{\frac{1}{\Theta_g}} = P \left(\frac{\sum_{h\in g}\left(-\frac{1}{\Theta_h^2}\frac{\mathrm{d}\Theta_h}{\mathrm{d}P}\Phi_h + \frac{1}{\Theta_h}\frac{\mathrm{d}\Phi_h}{\mathrm{d}P}\right)}{\sum_{h\in g}\frac{1}{\Theta_h}\Phi_h} - \frac{1}{\sum_{h\in g}\Phi_h}\sum_{h\in g}\frac{\mathrm{d}\Phi_h}{\mathrm{d}P} \right), \tag{24}$$

Based on the definition of a sensitivity coefficient we again have

$$\begin{aligned} \frac{\mathrm{d}\Theta_h}{\mathrm{d}P} &= \frac{\Theta_h}{P} S_P^{\Theta_h} \\ \frac{\mathrm{d}\Phi_h}{\mathrm{d}P} &= \frac{\Phi_h}{P} S_P^{\Phi_h}, \end{aligned}$$

which leads to

$$S_P^{\frac{1}{\Theta_g}} = P \left(\frac{\sum_{h\in g}\left(-\frac{1}{\Theta_h^2}\frac{\Theta_h}{P}S_P^{\Theta_h}\Phi_h + \frac{1}{\Theta_h}\frac{\Phi_h}{P}S_P^{\Phi_h}\right)}{\sum_{h\in g}\frac{1}{\Theta_h}\Phi_h} - \frac{1}{\sum_{h\in g}\Phi_h}\sum_{h\in g}\frac{\Phi_h}{P}S_P^{\Phi_h} \right) \tag{25}$$

and finally

$$S_P^{\frac{1}{\Theta_g}} = \frac{\sum_{h\in g}\left(-\frac{1}{\Theta_h}S_P^{\Theta_h}\Phi_h + \frac{1}{\Theta_h}\Phi_h S_P^{\Phi_h}\right)}{\sum_{h\in g}\frac{1}{\Theta_h}\Phi_h} - \frac{1}{\sum_{h\in g}\Phi_h}\sum_{h\in g}\Phi_h S_P^{\Phi_h} \tag{26}$$

or

$$S_P^{\frac{1}{\Theta_g}} = \frac{\sum_{h\in g}\frac{1}{\Theta_h}\Phi_h\left(S_P^{\Phi_h} - S_P^{\Theta_h}\right)}{\sum_{h\in g}\frac{1}{\Theta_h}\Phi_h} - \frac{\sum_{h\in g}\Phi_h S_P^{\Phi_h}}{\sum_{h\in g}\Phi_h}. \tag{27}$$

To obtain the sensitivity of Θ_g we'll simply multiply the previous expression by -1 (Eq. 2):

$$S_P^{\Theta_g} = -\frac{\sum_{h\in g} \frac{1}{\Theta_h}\Phi_h \left(S_P^{\Phi_h} - S_P^{\Theta_h}\right)}{\sum_{h\in g} \frac{1}{\Theta_h}\Phi_h} + \frac{\sum_{h\in g} \Phi_h S_P^{\Phi_h}}{\sum_{h\in g} \Phi_h}. \tag{28}$$

This is rather similar to the direct condensation (Eq. 19), but with some distinct differences.

4.3 Simple homogenized reaction cross sections

The sensitivity coefficients for the **absorption** and **fission cross sections** as well as the **inverse velocities** can be calculated directly as reaction rate ratios where the response is

$$R = \frac{\langle x, \phi\rangle_g}{\langle 1, \phi\rangle_g}$$

where x is one of the following: Σ_a, Σ_f or $1/v$. The calculation of these sensitivities can be achieved through setting up detectors for the reaction rate (the numerator) and the flux (the denominator).

Absorption cross section cannot currently be directly used as a detector response in Serpent, which means that the sensitivity for the absorption cross section needs to be calculated from the sensitivities of capture and fission cross sections and flux according to Eq. 5. Another possibility is to implement a separate detector response for the absorption cross section.

Serpent already has a detector response for $1/v$ but if the inverse velocity detector needs to only score prompt neutrons, some additional work is needed. This could be achieved by implementing a separate detector option to choose whether all or only prompt or delayed neutrons are scored.

The sensitivity of the **slowing down cross section** needs to be evaluated as a detector ratio

$$R = \frac{\langle \Sigma_{1\to 2}, \phi\rangle}{\langle 1, \phi\rangle}.$$

There is no implicit way to score the slowing down reaction rate in the numerator, which means that an analog estimator needs to be used for it. The slowing down reaction rate is not currently available as a detector response.

4.4 Other homogenized macroscopic cross sections

The sensitivity of the **fission production cross section** is slightly more complicated to calculate as both the nubar and the fission cross section may be uncertain (have covariance data). As the homogenized fission production cross section is simply

$$R = \frac{\langle \nu\Sigma_f, \phi\rangle}{\langle 1, \phi\rangle}$$

we know (Eq. 12) that its sensitivity contains both direct and indirect terms:

$$S_P^{\nu\Sigma_f} = \frac{\left\langle \frac{\partial(\nu\Sigma_f)}{\partial P/P}, \phi \right\rangle}{\langle \nu\Sigma_f, \phi\rangle} - \frac{\left\langle \frac{\partial 1}{\partial P/P}, \phi \right\rangle}{\langle 1, \phi\rangle} + \frac{\left\langle \nu\Sigma_f, \frac{\partial \phi}{\partial P/P} \right\rangle}{\langle \nu\Sigma_f, \phi\rangle} - \frac{\left\langle 1, \frac{\partial \phi}{\partial P/P} \right\rangle}{\langle 1, \phi\rangle}. \tag{29}$$

The second direct term will be zero due to the derivative term in the numerator being zero:

$$S_P^{\nu\Sigma_f} = \frac{\left\langle \frac{\partial(\nu\Sigma_f)}{\partial P/P}, \phi \right\rangle}{\langle \nu\Sigma_f, \phi \rangle} + \frac{\left\langle \nu\Sigma_f, \frac{\partial\phi}{\partial P/P} \right\rangle}{\langle \nu\Sigma_f, \phi \rangle} - \frac{\left\langle 1, \frac{\partial\phi}{\partial P/P} \right\rangle}{\langle 1, \phi \rangle}. \tag{30}$$

The calculation of the sum of the indirect terms has been previously implemented into Serpent. However, in the case of the direct term the evaluation of the derivative $\frac{\partial(\nu\Sigma_f)}{\partial P}$ necessitates working it into

$$\frac{\partial(\nu\Sigma_f)}{\partial P/P} = P\left(\frac{\partial\nu}{\partial P}\Sigma_f + \nu\frac{\partial\Sigma_f}{\partial P}\right) \tag{31}$$

In practice, the perturbation P is either ν, Σ_f or something else (such as $\Sigma_{s,\text{ela}}$). If the perturbation is the nubar, i.e. we are calculating the sensitivity of the fission production cross section to perturbations in ν the derivative will yield

$$\frac{\partial(\nu\Sigma_f)}{\partial P/P} = \nu\left(\frac{\partial\nu}{\partial\nu}\Sigma_f + \nu\frac{\partial\Sigma_f}{\partial\nu}\right) = \nu\Sigma_f \tag{32}$$

meaning that the sensitivity coefficient is

$$S_\nu^{\nu\Sigma_f} = \frac{\langle \nu\Sigma_f, \phi \rangle}{\langle \nu\Sigma_f, \phi \rangle} + \frac{\left\langle \nu\Sigma_f, \frac{\partial\phi}{\partial P/P} \right\rangle}{\langle \nu\Sigma_f, \phi \rangle} - \frac{\left\langle 1, \frac{\partial\phi}{\partial P/P} \right\rangle}{\langle 1, \phi \rangle}. \tag{33}$$

If, on the other hand $P = \Sigma_f$ we have

$$\frac{\partial(\nu\Sigma_f)}{\partial P/P} = \Sigma_f\left(\frac{\partial\nu}{\partial\Sigma_f}\Sigma_f + \nu\frac{\partial\Sigma_f}{\partial\Sigma_f}\right) = \nu\Sigma_f \tag{34}$$

yielding the same sensitivity coefficient

$$S_{\Sigma_f}^{\nu\Sigma_f} = \frac{\langle \nu\Sigma_f, \phi \rangle}{\langle \nu\Sigma_f, \phi \rangle} + \frac{\left\langle \nu\Sigma_f, \frac{\partial\phi}{\partial P/P} \right\rangle}{\langle \nu\Sigma_f, \phi \rangle} - \frac{\left\langle 1, \frac{\partial\phi}{\partial P/P} \right\rangle}{\langle 1, \phi \rangle}. \tag{35}$$

For these two perturbations the direct term is simply 1 whereas if the perturbation is something not related to ν or Σ_f the derivative in the numerator of the direct term will be zero yielding zero for the first term. As fission neutron production is available as a detector response function in Serpent, the only additional work required is the implementation of the calculation of the direct term of the reaction rate sensitivity.

The **fission poison production cross section** sensitivities can be calculated in a manner similar to the fission neutron production sensitivity with

$$R = \frac{\langle \gamma\Sigma_f, \phi \rangle}{\langle 1, \phi \rangle}$$

where $\gamma\Sigma_f$ is the fission yield of the fission poison summed up from the fissile actinides as

$$\gamma\Sigma_f = \sum_y \gamma_y \Sigma_{f,y}$$

with $\Sigma_{f,y}$ being the macroscopic fission cross section of a specific actinide and γ_y being the fission yield for the fission poison (including immediate precursors) from a fission of actinide y. Currently, the macroscopic fission yield of a fission poison is not available as a detector response function in Serpent meaning that the calculation of the sensitivity is possible only after the response function is implemented or if the sensitivity is calculated manually[2] in `scorepoison.c`.

The sensitivity for **energy per fission** can also be calculated in a similar manner with

$$R = \frac{\langle \kappa\Sigma_f, \phi \rangle}{\langle \Sigma_f, \phi \rangle}$$

where κ is the fission energy productions. This is a simple reaction rate ratio where both the reaction rates can already be tallied with Serpent (dr -8 for fission energy deposition and dr -6 for fission rate).

4.5 Homogenized microscopic cross sections

Homogenized microscopic absorption cross sections for nuclide x are calculated by Serpent as

$$\sigma_{a,g,x} = \frac{V}{V_f} \frac{\int_{V_f} \int_{E_g}^{E_{g-1}} \sigma_{a,x}(E)\phi(\vec{r}, E)\mathrm{d}E\mathrm{d}^3 r}{\int_V \int_{E_g}^{E_{g-1}} \phi(\vec{r}, E)\mathrm{d}E\mathrm{d}^3 r} \tag{36}$$

where V_f refers to the volume of the fuel region. In this case the response is

$$R = \frac{V}{V_f} \frac{\langle \sigma_{a,x}, \phi \rangle}{\langle 1, \phi \rangle}$$

and based on Eq. 7, the constant multiplier of V/V_f need not be considered when evaluating the sensitivity. It suffices to calculate the sensitivity of

$$R = \frac{\langle \sigma_{a,x}, \phi \rangle}{\langle 1, \phi \rangle}$$

which is a simple reaction rate ratio. Both the microscopic reaction rate in the numerator and the flux in the denominator can be calculated with normal Serpent detectors. The integration area of the microscopic reaction rate needs to be limited to fuel materials. The calculation of any homogenized microscopic cross sections can thus be achieved without additional implementations.

[2] i.e. not as a detector ratio

4.6 Diffusion coefficient

The generation of feasible **diffusion coefficients** with Monte Carlo codes is generally considered to be a complex problem and various different approaches for calculating the diffusion coefficient exist.

For example, one of the approaches used by Serpent based on the out-scatter approximation [7] calculates the diffusion coefficient as

$$D_g = \frac{\sum_{h \in g} \frac{1}{3\Sigma_{\mathrm{tr},h}} \Phi_h}{\sum_{h \in g} \Phi_h} \tag{37}$$

where $\Sigma_{\mathrm{tr},h}$ and Φ_h are the (intermediate) multi-group estimates for the out-scatter transport cross section and group flux in group h respectively. To write this in a bit simpler format, we'll say that

$$D_g = \frac{1}{3} \frac{1}{\Sigma_{\mathrm{tr},g}}, \tag{38}$$

where

$$\frac{1}{\Sigma_{\mathrm{tr},g}} = \frac{\sum_{h \in g} \frac{1}{\Sigma_{\mathrm{tr},h}} \Phi_h}{\sum_{h \in g} \Phi_h}. \tag{39}$$

In order to calculate the sensitivity coefficient for D_g we can write

$$S_p^{D_g} = S_P^{\frac{1}{3}\frac{1}{\Sigma_{\mathrm{tr},g}}}$$

since a constant multiplier does not affect the sensitivity (Eq. 7) this is

$$S_p^{D_g} = S_P^{\frac{1}{\Sigma_{\mathrm{tr},g}}} = -S_P^{\Sigma_{\mathrm{tr},g}}.$$

We can use the formula for the inverse condensation of the sensitivity coefficient (Eq. 28) to obtain $S_P^{\Sigma_{\mathrm{tr},g}}$ from $S_P^{\Sigma_{\mathrm{tr},h}}$ and $S_P^{\phi_h}$, i.e. from the multi-group sensitivities of the transport cross section and the flux. The out-scatter transport cross section is calculated as

$$\Sigma_{\mathrm{tr},h} = \Sigma_{\mathrm{tot},h} - \Sigma_{\mathrm{s1},h} \tag{40}$$

where $\Sigma_{\mathrm{s1},h}$ is an analog estimate for

$$\Sigma_{\mathrm{s1},h} = \frac{\int_V \int_{E_h}^{E_{h-1}} \int_{E_{\min}}^{E_{\max}} \mu(E \to E') \Sigma_s(\vec{r}, E \to E') \phi(\vec{r}, E) \mathrm{d}E' \mathrm{d}E \mathrm{d}^3 r}{\int_V \int_{E_h}^{E_{h-1}} \phi(\vec{r}, E) \mathrm{d}E \mathrm{d}^3 r}, \tag{41}$$

i.e. group h's flux-weighted spatial and energy averaging of the scattering cross section times the scattering cosine.

As the transport cross section is defined (Eq. 40) as a difference between the total cross section and the P1-scattering cross section its sensitivity can be calculated from the values and sensitivities of the two component cross sections (based on Eq. 6):

$$S_P^{\Sigma_{\text{tr}}} = \frac{\Sigma_{\text{tot}}}{\Sigma_{\text{tot}} - \Sigma_{\text{s1}}} S_P^{\Sigma_{\text{tot}}} - \frac{\Sigma_{\text{s1}}}{\Sigma_{\text{tot}} - \Sigma_{\text{s1}}} S_P^{\Sigma_{\text{s1}}}. \tag{42}$$

Calculating the sensitivity coefficient for the out-scatter diffusion coefficient requires the calculation of the sensitivity for both the total cross section, which is straightforward, and the P1-scattering cross section, which is slightly more complicated.

The response is

$$R = \frac{\langle \mu \Sigma_s, \phi \rangle}{\langle 1, \phi \rangle},$$

which can be calculated as a reaction rate ratio similar to the homogenized fission neutron, poison or energy production cross section (see Section 4.4) with care put into evaluating the direct term of the sensitivity. As the energy dependent mean scattering cosine is generally not available, the detector in the numerator needs to be scored in an analog manner.

The sensitivity of this diffusion coefficient can thus be calculated if estimates are found for the sensitivities of the multi-group flux, total cross section and P1 scattering cross section. The P1 scattering cross section is currently not available as a detector response function.

Serpent does offer several alternate methods for calculating the diffusion coefficient some of which may be more straightforward to include in the sensitivity calculation. The transport corrected diffusion coefficient (`TRC_DIFFCOEF`) also calculates the diffusion coefficient as

$$D_g = \frac{1}{3} \frac{1}{\Sigma_{\text{tr},g}},$$

but instead of using the P1 scattering cross section in calculating the transport correction to the total cross section it uses a user given energy dependent transport correction

$$f(E) = \frac{\Sigma_{\text{tr}}(E)}{\Sigma_{\text{tot}}(E)}$$

to calculate the transport cross section directly from the total cross section. As the P1 scattering cross section does not need to be tallied the sensitivity for the transport corrected diffusion coefficient can be calculated without additional implementations.

4.7 Discontinuity factors

If the homogenized region covers the whole of the simulated geometry and the homogenization is performed using reflective boundary conditions the **discontinuity factors** for surface S_k can be calculated from (see Eq. 28 of [7]):

$$F_{g,k} = \frac{\frac{1}{S_k} \int_{S_k} \int_{E_g}^{E_{g-1}} \phi(\vec{r}, E) \mathrm{d}E \mathrm{d}^2 r}{\frac{1}{V} \int_V \int_{E_g}^{E_{g-1}} \phi(\vec{r}, E) \mathrm{d}E \mathrm{d}^3 r} \tag{43}$$

The numerator can be evaluated using a surface flux detector while the denominator is evaluated through the use of a volumetric flux detector. Discontinuity factors can thus be seen

as simple detector ratios and their sensitivities can be calculated using the formula for detector ratio sensitivities. It should be noted, however that the scoring of surface based detectors in Serpent is done separately from (volumetric) collision detectors, which requires further changes in order to extend the sensitivity capabilities to cover surface detectors. The constant multiplier V/S_k can be ignored as per Eq. 7 when calculating the sensitivity.

If, the homogenized region is simply a subset of the simulated geometry (e.g. colorset/reflector homogenization) the discontinuity factors need to be solved from a diffusion equation formulated for the homogenized region using the boundary (and corner) net currents tallied in the heterogeneous calculation as a boundary condition. It is most likely possible to obtain estimates for the sensitivities (or uncertainties) of the different terms appearing in the homogeneous diffusion equation without much additional work but propagating the sensitivities (or uncertainties) to the solution of the homogeneous diffusion equation is not straightforward and needs to be considered in the future.

4.8 Albedos

The **total albedo matrix** produced by Serpent is calculated by tallying the ratio of two surface current detectors

$$\alpha_{gg',k} = \frac{\int_{E_g'}^{E_{g'-1}} \int_{S_k} \vec{J}_g^-(\vec{r},E)\cdot \mathrm{d}\vec{S}\mathrm{d}E}{\int_{E_g}^{E_{g-1}} \int_{S_k} \vec{J}^+(\vec{r},E)\cdot \mathrm{d}\vec{S}\mathrm{d}E}, \tag{44}$$

where $\vec{J}^+$ is the escaping current and $\vec{J}_g^-(\vec{r},E)$ is the returning current formed by neutrons that left the active core in group g. A sensitivity can be calculated for the ratio of two surface detectors in a straightforward manner. Partial neutron currents are already available as detector response functions in Serpent.

The **partial albedos** are calculated for a non-multiplying volume as

$$\alpha_{gg',kk'} = \frac{\int_{E_g'}^{E_{g'-1}} \int_{S_{k'}} \vec{J}_{g,k}^-(\vec{r},E)\cdot \mathrm{d}\vec{S}\mathrm{d}E}{\int_{E_g}^{E_{g-1}} \int_{S_k} \vec{J}^+(\vec{r},E)\cdot \mathrm{d}\vec{S}\mathrm{d}E}, \tag{45}$$

where $\vec{J}_{g,k}^-$ is the outward current component formed by neutrons that have entered the non-multiplying volume in energy group g through face k and exit the volume in energy group g' through face k'. Again, the estimate is calculated as a ratio of two detectors and the sensitivity can be calculated in a standard manner.

4.9 Group-wise delayed neutron fractions

The calculation of the total effective delayed neutron fraction β_{eff} is one of the existing capabilities of Serpent. Calculating sensitivities for the group-wise data $\beta_{\mathrm{eff},i}$ requires small additional implementations where the sensitivity for each group is calculated separately. Serpent actually outputs the $\beta_{\mathrm{eff},i}$ calculated using multiple methods. The sensitivities are calculated for the IFP-based method (`ADJ_IFP_ANA_BETA_EFF`).

4.10 Delayed neutron group wise decay constants

The calculation of the sensitivities for the delayed neutron decay constants is not one of the existing capabilities, but for the IFP-based decay constants (`ADJ_IFP_ANA_LAMBDA`) the calculation of the sensitivity can be achieved in a manner rather similar to the group-wise delayed neutron fraction. The extension of the capability to the group-wise decay constants should be simple.

It should be noted that in the JEFF-libraries the delayed neutron group structure is the same for every fissionable nuclide, which means that the group wise decay constants are the same for the homogenized system and insensitive to perturbations in nuclear data[3]. In ENDF/B and JENDL-libraries, however each fissionable nuclide has their own six group delayed neutron group structure. The six homogenized decay constants are thus different from the nuclide-wise decay constants and thus may be sensitive to perturbations in the nuclear data.

[3] other than the decay constants themselves

5. Extending Serpent for uncertainty propagation

This section describes the practical new implementations that were achieved during this work.

5.1 Reading in covariance data

In order to provide statistical uncertainty information on the calculated nuclear data uncertainties the Sandwich rule (Eq. 8) needs to be applied for each neutron batch separately using the sensitivity coefficients calculated for that batch. This requires Serpent to read in covariance data for the nuclear data for which the uncertainties are to be produced.

Two widely used multigroup covariance data formats for nuclear data are the COVERX format used by SCALE [8] and the Boxer format used produced by the COVR module of NJOY [9]. As the covariance data distributed with the SCALE code system has been widely used in benchmarking calculations in the UAM-benchmark, reading routines were first implemented for the COVERX data format to allow for code-to-code comparisons with previously published results. Support for the output format of COVR can be added in the future.

Readers were implemented for both the binary format of COVERX used by the 56 and 252 group covariance data libraries distributed with SCALE-6.2 and for the ASCII format of COVERX used by the 44 group covariance data libraries distributed with SCALE-6.0.

The reader routines were verified by comparing the covariance data read by Serpent to covariance data read from the binary COVERX files using the C++ utilities distributed with SCALE-6.2.1 (`CoverXReader.cpp`).

5.2 Processing the covariance data into a suitable format

After the covariance data is read to Serpent the data is collected either as connected nuclide/reaction mode blocks such as that shown in Fig. 2 for the covariances of the reaction modes of ^{155}Gd or as separate single reaction mode blocks such as those shown in Fig. 3 for the same covariances of ^{155}Gd. The sandwich rule will be applied to each of these blocks separately and the covariance from each block can be evaluated separately.

During this process, the covariance matrices are made symmetrical by averaging the upper and lower triangular parts of each matrix. The covariance matrices should be symmetric and positive-semidefinite by definition, but the output of processing codes is not always such.

In the future, the covariance data could be pre-processed using the practices described in [10] in order to ensure the consistency and positive-semidefiniteness of the covariance matrices. However, this requires some additional linear algebra such as eigendecompositions for which methods are currently not found in Serpent.

5.3 Calculating the sensitivities of sum reaction modes

In some cases, the nuclear covariance data is available for a sum reaction mode, e.g. MT 4 (inelastic scattering) while the cross section data used for neutron transport does not contain this sum reaction mode and instead includes the partial reaction modes (e.g. MT 51-91). For such cases, the sensitivities are calculated separately for the partial reaction modes and the sensitivity is summed up internally, whenever some subroutine requests the sensitivity of the sum reaction mode. This applies to inelastic scattering (MT 4 summed up from MT 51-91),

fission (MT 18 summed up from MT 19-21), nubar (MT 452 summed up from MT 455 and 456) and fission spectrum (total fission spectrum summed up from prompt and delayed).

A similar kind of an internal summation is also conducted when subroutines request sensitivities summed up over all energies, materials, nuclides or reaction modes.

5.4 Calculating the direct term of detector sensitivities

The direct term of detector sensitivities

$$\frac{\left\langle \frac{\partial \Sigma_i}{\partial P/P}, \phi \right\rangle}{\langle \Sigma_i, \phi \rangle} \tag{46}$$

describes the relative change in the sensitivity response (detector value) due to a relative change in the detector response function due to the applied perturbation P. Generally, the calculation of this term depends on whether the perturbation P is:

1. The detector response function Σ_i.
2. A partial reaction mode of Σ_i.
3. Unrelated to Σ_i.

In the first case the direct term is simply

$$\frac{\left\langle \frac{\partial \Sigma_i}{\partial \Sigma_i/\Sigma_i}, \phi \right\rangle}{\langle \Sigma_i, \phi \rangle} = \frac{\left\langle \Sigma_i \frac{\partial \Sigma_i}{\partial \Sigma_i}, \phi \right\rangle}{\langle \Sigma_i, \phi \rangle} = \frac{\langle \Sigma_i, \phi \rangle}{\langle \Sigma_i, \phi \rangle} = 1. \tag{47}$$

In the second case we have $P = \Sigma_j$ and

$$\Sigma_i = \Sigma_j + \sum_k \Sigma_k \tag{48}$$

where Σ_k are the cross sections of the other partial reaction modes that are included in Σ_i. This gives us the following direct term

$$\frac{\left\langle \frac{\partial \Sigma_i}{\partial \Sigma_j/\Sigma_j}, \phi \right\rangle}{\langle \Sigma_i, \phi \rangle} = \frac{\left\langle \Sigma_j \frac{\partial}{\partial \Sigma_j} \left(\Sigma_j + \sum_k \Sigma_k \right), \phi \right\rangle}{\langle \Sigma_i, \phi \rangle} = \frac{\langle \Sigma_j, \phi \rangle}{\langle \Sigma_i, \phi \rangle}, \tag{49}$$

which is simply the relative contribution of the j partial reaction mode to the detector value for the sum reaction mode i.

In the third case, the detector response does not depend on the perturbed quantity resulting in the derivative in Eq. 46 being zero and yielding zero as the direct term.

In an ideal situation our perturbations would fall only into categories 1 and 3 and have our direct term be always one or zero. However, the homogenized reaction cross sections used by reduced order solvers are typically for sum reaction mode (e.g. Σ_{abs} or Σ_{fiss}) while the covariance data is given for partial reaction modes (radiative capture, first chance fission, second chance fission etc.).

In order to calculate the direct term in Eq. 49 during the simulation both

$$\langle \Sigma_j, \phi \rangle$$

and

$$\langle \Sigma_i, \phi \rangle$$

need to be evaluated. The latter term is simply the detector value and will be calculated automatically. The former term is the reaction rate of reaction j in the integration domain of the detector and such terms will tallied through the following means:

In order to keep the integration domain of the partial reaction rate ($\langle \Sigma_j, \phi \rangle$) equal to that of the detector reaction rate ($\langle \Sigma_i, \phi \rangle$) the partial reaction rate will be scored if and only if the detector reaction rate is scored. If a detector reaction rate is scored for a detector included in a sensitivity calculation, Serpent will first check whether the reaction rate being tallied is one of the following

- Total reaction rate.
- Total capture rate.
- Total fission rate.
- Total elastic scattering rate.
- Total fission neutron production rate.

In such cases, Serpent will score the partial reaction rate separately for all of the reactions that are **both** listed as partial reactions of the detector response **and** being perturbed in the sensitivity calculation. This will score all of the relevant partial reaction rates for the detector.

The direct sensitivities are thus calculated during the Serpent run and added to the indirect sensitivities to yield the total sensitivities to be both used for the uncertainty propagation and output as the detector sensitivities. As indicated by the preceding list, the direct sensitivities are currently calculated for Σ_{tot}, Σ_c, Σ_f, $\Sigma_{s,\text{ela}}$ and $\nu\Sigma_f$.

5.5 Adding support for surface detectors

In the previous implementation, the detector ratio sensitivity responses could only include detectors scored in `coldet.c`. The calculation of sensitivities for the discontinuity factors and albedos required adding support for surface detectors scored in `superdet.c`.

After this extension, the user can also use surface detectors (defined with detector option **ds**) in detector ratio responses.

5.6 Adding support for multi-bin detectors

Previously, the detector ratio sensitivities have been calculated only for detectors with a single bin. For example, the calculation of sensitivities for thermal and fast fission cross section has required separate detectors for thermal fission rate, fast fission rate, thermal flux and fast flux. This will soon become problematic if sensitivities are to be calculated for multi-group cross sections instead of few-group cross sections.

Serpent supports the linking of an energy grid to a detector definition, which allows the user to calculate the detector response in each group using a single detector definition. In order to easily calculate multi-group sensitivities it would be beneficial to simply allow the user to define

the response as a ratio of two such multi-bin detectors. Actually, the interesting responses in this case are the bin-wise ratios between the two detectors (bin 1 of detector 1 divided by bin 1 of detector 2 etc.).

Serpent was thus extended to accept detector ratio responses of two detectors with multiple bins. The number of bins in the two detectors must be equal and each detector may have at most one response defined with the "`dr`"-option.

After the extension, Serpent will "split" the initially defined detector ratio response into new responses covering the bin-wise ratios of the two detectors.

The implementation was verified by comparing the two-group sensitivities calculated using the old implementation and single bin detectors to ones obtained with the new implementation and two energy bin detectors.

The implementation is not limited to energy-bins but covers also spatial bins.

5.7 Adding support for group-wise delayed neutron fraction sensitivities

The previous implementation of the sensitivity routines only calculated the sensitivity of total β_{eff}. As group-wise delayed neutron fractions are needed for HEXTRAN/TRAB3D the methodology was extended to also calculate the sensitivities for the group-wise delayed neutron fractions.

The sensitivities and uncertainties for the group-wise delayed neutron fractions can now be set to be calculated separately from the total fraction with "`sens resp beff <total> <groupwise>`" where `<total>` and `<groupwise>` are flags (0/1/no/yes) indicating whether the calculation should be turned off or on.

5.8 Adding support for group-wise decay constant sensitivities

The previous implementation of the sensitivity routines did not calculate the sensitivity for the delayed neutron precursor group decay constants. This was added as an option switched on with "`sens resp lambda <total> <groupwise>`" where `<total>` and `<groupwise>` are flags (0/1/no/yes) indicating whether the calculation should be turned off or on. The methodology relies on calculating the sensitivity for λ as a bilinear ratio of adjoint-weighted quantities (see Section 5 of [6]) and the sensitivity is calculated as

$$S_x^{\lambda_{\text{eff}}} = \frac{E\left[{}^{(-\gamma)}\lambda \cdot \sum^{\text{history}} (\text{ACC}_x - \text{REJ}_x)\right]}{E\left[{}^{(-\gamma)}\lambda\right]} - E\left[\sum^{\text{history}} (\text{ACC}_x - \text{REJ}_x)\right], \tag{50}$$

where the λ is the delayed neutron group decay constant and the other notation follows that of Eq. 37 of [6] where the sensitivity for prompt neutron lifetime was derived.

5.9 Applying the sandwich rule

The sandwich rule is applied for each separate covariance block after each neutron batch according to Eq. 8. The correct sensitivity vectors $\overline{\mathbf{S}}_X^R$ are first collected from the sensitivity results based on the reaction mode(s) included in the covariance block. The vector-matrix-vector multiplication is then conducted and the square root of the resulting covariance is stored as the uncertainty coming from that specific covariance block. The covariances from the different

blocks are summed up to produce the total covariance in the response and the square root is stored as the total nuclear data uncertainty of the response. The process is repeated for each response R.

6. Results and comparisons

In this section, some example results are presented and some assembly level results are compared to similar results obtained previously using CASMO-4E. These comparisons cannot be considered to yet constitute a thorough validation of the capabilities as the output uncertainties necessarily depend both on the used transport solver and the utilized covariance data. The best reference solution that could be used for validating the capabilities would be a sampling based method, where the cross section data is actually perturbed based on the multi-group covariance data to produce hundreds or thousands of cross section data libraries. These data libraries can then be used for Serpent calculations and the nuclear data uncertainties of various output quantities can be inferred from the statistical spread of the output quantities in this group of calculations.

For the calculations shown here, the output group constants were calculated as detector ratios using directly the two-group energy structure. The utilization of the direct and inverse energy group condensations of the sensitivities (Eq. 19 and Eq. 28) needs to be implemented at a future time.

These calculations focus on group constants instead of time-constants. The β_{eff} sensitivities calculated by Serpent have previously been verified in code-to-code comparisons in [12].

The calculations used the 56 group covariance library distributed with SCALE-6.2. The covariance library was linked to the Serpent calculation with the new input option

```
set coverxlib "/home/vvvillehe/XSdata/scale.rev08.56groupcov7.1"
```

6.1 Pin-cells

The pin-cell test cases included the Peach Bottom 2 and Three Mile Island 1 pin-cells from the UAM-benchmark phase I specifications [13].

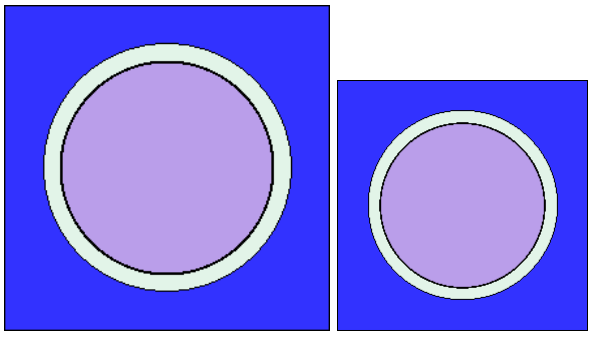

Figure 5. Peach Bottom 2 and Three Mile Island 1 pin-cell geometries to scale with each other.

The two pin-cell geometries are shown in Fig. 5. The fuel in the BWR pin-cell had a lower enrichment than the one in the PWR pin-cell (2.93 wt.% vs. 4.85 wt.%). While the HZP thermal hydraulic conditions were similar between the two pin-cells the BWR HFP case had a 40 % void fraction compared to the 0 % void fraction of the HFP PWR pin-cell.

Both HZP and HFP conditions were calculated for both pin-cells.

6.1.1 Considered responses

The responses for which the nuclear data uncertainty was calculated are based on the UAM-problem definition:

- Effective multiplication factor (k_{eff})
- Microscopic one-group fission cross sections for ^{235}U and ^{238}U.
- Microscopic one-group absorption cross sections for ^{235}U and ^{238}U.
- Macroscopic one-group fission cross section.
- Macroscopic one-group absorption cross section.

As the new implementation propagates the nuclear data uncertainties automatically for each response for which sensitivities are calculated it was enough to simply set up a sensitivity calculation for each of the responses. This was achieved with the following inputs:

Effective multiplication factor:

The calculation of the effective multiplication factor can be switched on using

```
sens resp keff
```

Microscopic one-group cross sections

The UAM-benchmark specifications do not specify how the microscopic one-group cross sections should be calculated (e.g. integration volumes). Here we conduct the homogenization according to Eq. 36, i.e. by using the fuel volume as the homogenization volume for the microscopic reaction rate and the whole geometry volume to calculate the homogeneous flux:

We'll first specify the materials representing ^{235}U and ^{238}U:

```
mat U5 1.0
92235.09c 1.0

mat U8 1.0
92238.09c 1.0
```

Then we'll set up detectors for the one-group microscopic fission and capture rates in the fuel region as well as the total one-group flux in the whole geometry:

```
det C5      dr -2 U5 dm fuel
det F5      dr -6 U5 dm fuel
det C8      dr -2 U8 dm fuel
det F8      dr -6 U8 dm fuel
det FLX
```

Finally, we'll specify the ratios of the reaction rates and flux as sensitivity responses in order to obtain the sensitivities and the uncertainties for the cross sections:

```
sens resp detratio 5FISXS F5 FLX
sens resp detratio 8FISXS F8 FLX
sens resp detratio 5CPTXS C5 FLX
sens resp detratio 8CPTXS C8 FLX
```

We will calculate the sensitivity/uncertainty of the microscopic absorption cross section based on the microscopic capture and fission cross sections using Eq. 5.

Macroscopic one-group cross sections

We will simply set up detectors for the one-group macroscopic fission and capture rates as well as the total one-group flux (in fact the total one-group flux detector is the one we defined for the homogenized microscopic cross sections):

```
det FIS     dr -6 void
det CPT     dr -2 void
det FLX
```

Then, we'll specify the ratios of the macroscopic reaction rates and flux as sensitivity responses in order to obtain the sensitivities and the uncertainties for the cross sections:

```
sens resp detratio FISXS  FIS FLX
sens resp detratio CPTXS  CPT FLX
```

6.1.2 Results

The homogenized microscopic cross sections calculated as a ratio of the microscopic reaction rate in the fuel region and volumetric flux detector values needed to be scaled by the V/V_f term in Eq. 36, i.e. the ratio between unit-cell volume and fuel volume.

The hot full power results are shown in the following Tables (1 and 2), whereas the HZP-results are tabulated in Appendix A. As the values of the group coefficients were calculated from the reaction rates and fluxes in a post-processing step, no information of their statistical uncertainty is available. This is also true for the nuclear data uncertainty of the macroscopic absorption cross section which was calculated from the nuclear data uncertainties of the fission and capture cross sections.

The largest nuclear data uncertainties are found in the homogenized microscopic fission cross section for ^{238}U being 4.9 % for the TMI1 pin-cell and 5.7 % for the PB2 pin-cell. The main contributors to this uncertainty are the uncertainties in the fission spectrum of ^{235}U and in the inelastic scattering cross section of ^{238}U as seen from Fig. 6.

As a second example the top contributors to the uncertainty of the homogenized one-group fission cross section are shown in Fig. 7. The top contributors include the inelastic scattering cross section of ^{238}U, fission spectrum of ^{235}U, the capture cross sections of both uranium isotopes and the elastic scattering cross section of hydrogen.

It may be interesting to note that in the higher fuel enrichment system (TMI1, 4.85 wt.%) the uncertainties related to ^{235}U are pronounced compared to the lower enrichment case (PB2, 2.93 wt.%).

Table 1. TMI1 pin-cell HFP

Parameter	Value	Nuclear data uncertainty (percent) $\pm 2\sigma$ statistical uncertainty
k_{eff}	1.38802	0.56300 ± 0.00152
$\sigma_{c,5}$	0.88533	1.79426 ± 0.00269
$\sigma_{c,8}$	0.09181	1.51706 ± 0.00440
$\sigma_{a,5}$	4.61351	1.38244 ± 0.00000
$\sigma_{a,8}$	0.10314	1.89250 ± 0.00000
$\sigma_{f,5}$	3.72818	1.28465 ± 0.00385
$\sigma_{f,8}$	0.01133	4.93548 ± 0.00543
Σ_c	0.01036	1.31425 ± 0.00302
Σ_a	0.02374	1.11684 ± 0.00000
Σ_f	0.01338	0.96396 ± 0.00357

Table 2. PB2 pin-cell HFP

Parameter	Value	Nuclear data uncertainty (percent) $\pm 2\sigma$ statistical uncertainty
k_{eff}	1.19005	0.72098 ± 0.00274
$\sigma_{c,5}$	0.82838	1.90970 ± 0.00382
$\sigma_{c,8}$	0.08167	1.56113 ± 0.00468
$\sigma_{a,5}$	4.24926	1.50763 ± 0.00000
$\sigma_{a,8}$	0.09128	1.99689 ± 0.00000
$\sigma_{f,5}$	3.42088	1.41027 ± 0.00592
$\sigma_{f,8}$	0.00961	5.69997 ± 0.00684
Σ_c	0.00849	1.38571 ± 0.00388
Σ_a	0.01636	1.13802 ± 0.00000
Σ_f	0.00787	0.87089 ± 0.00514

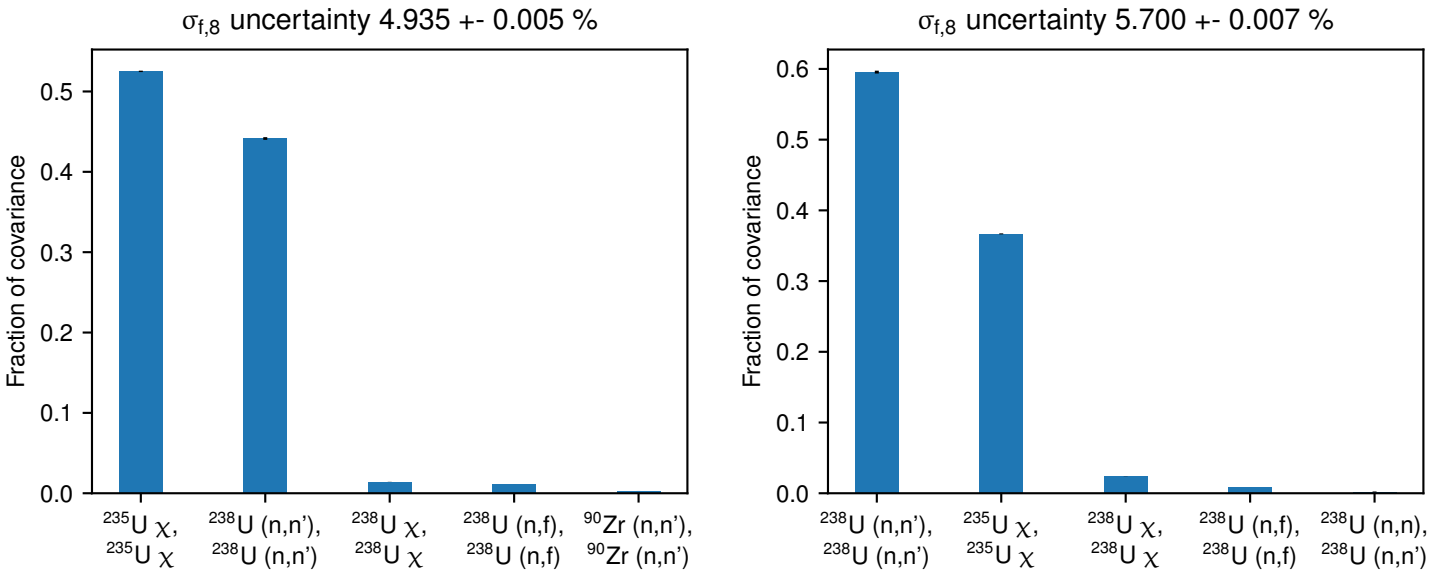

Figure 6. ***HFP pin-cells:*** *Top contributors (as a fraction of the total covariance) to the uncertainty of homogenized microscopic fission cross section of ^{238}U in the TMI1 pin-cell (**left**) and in the PB2 pin-cell (**right**).*

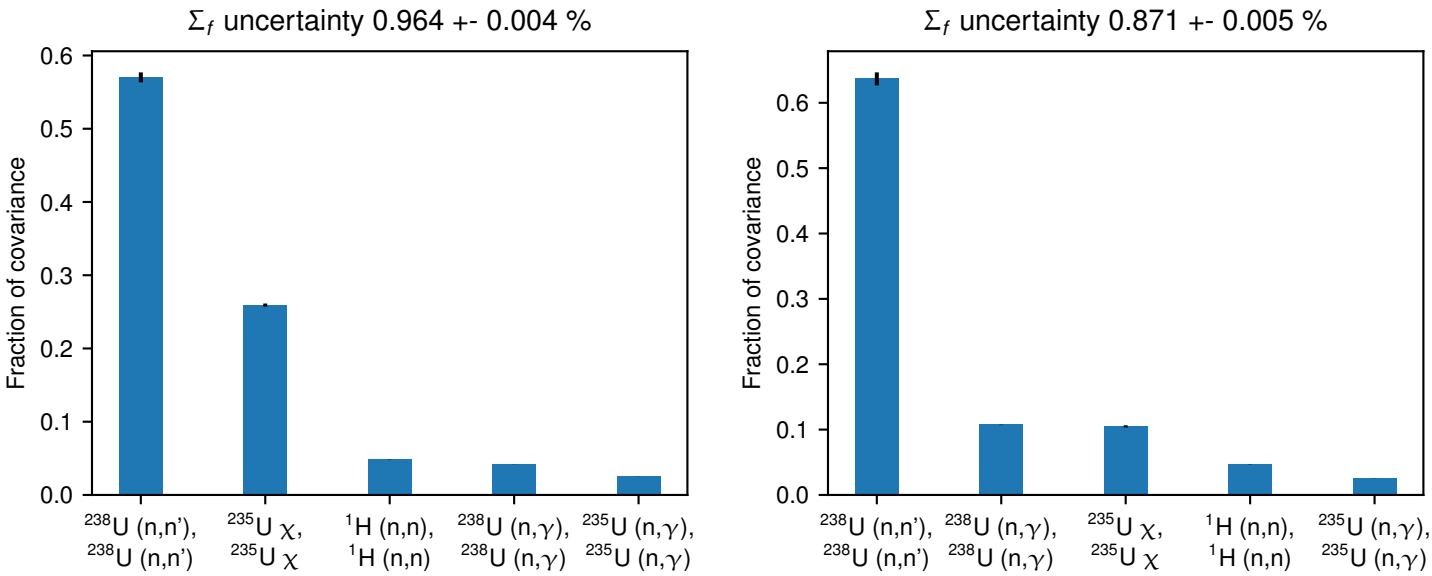

Figure 7. ***HFP pin-cells:*** *Top contributors (as a fraction of the total covariance) to the uncertainty of the homogenized macroscopic fission cross in the TMI1 pin-cell (**left**) and in the PB2 pin-cell (**right**).*

6.2 Assemblies

The single assembly test cases included the Peach Bottom 2 and Three Mile Island 1 assembly problems from the UAM-benchmark phase I specifications [13].

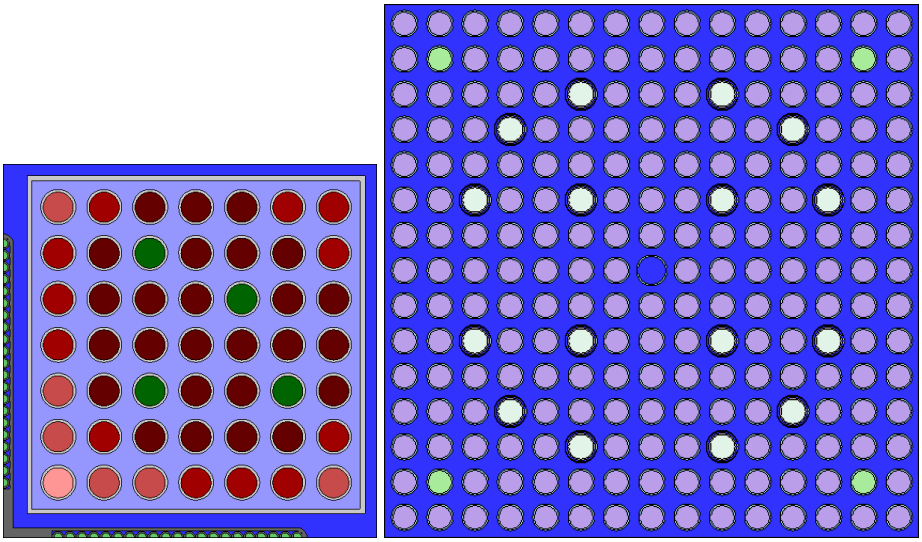

Figure 8. Rodded Peach Bottom 2 and Three Mile Island 1 assembly geometries to scale with each other.

The assembly geometries for the PB2 and TMI1 cases are shown in Fig. 8. The PB2 lattice contained five different fuel types one of which contained gadolinia as a burnable absorber (the rods indicated in green). A cruciform control rod with boron carbide as the absorber material could be included in the wide-wide corner of the geometry along the southern and western sides of the geometry. The TMI1 lattice contained two different fuel types one of which contained gadolinia as a burnable absorber (the rods indicated in green). Sixteen finger-type AIC control rods could be inserted into the guide tubes of the assembly.

Both HZP and HFP conditions for the unrodded and rodded geometries were modelled for both assemblies.

6.2.1 Considered responses

The responses for which the nuclear data uncertainty was calculated are based on the UAM-problem definition:

- Effective multiplication factor (k_{eff})
- Macroscopic two-group fission cross section.
- Macroscopic two-group absorption cross section.
- Macroscopic two-group elastic scattering cross section.
- Macroscopic two-group fission neutron production cross section.
- Two-group assembly discontinuity factors.

The calculation of the effective multiplication factor sensitivity/uncertainty is switched on as previously.

Macroscopic two-group cross sections

The sensitivities/uncertainties for the macroscopic two-group cross sections were calculated by first setting up a default two-group energy structure

```
ene myGS 1 1e-11 6.25e-7 2e1
```

adding the detectors for the two-group reaction rates and flux

```
det FIS     dr -6 void de myGS
det CPT     dr -2 void de myGS
det ELA     dr -3 void de myGS
det NSF     dr -7 void de myGS
det FLX                de myGS
```

and specifying the correct reaction rate ratios as sensitivity responses

```
sens resp detratio FISXS  FIS FLX
sens resp detratio CPTXS  CPT FLX
sens resp detratio ELAXS  ELA FLX
sens resp detratio NSFXS  NSF FLX
```

The sensitivity/uncertainty for the macroscopic absorption cross section for each group is again calculated from those of the macroscopic capture and fission cross sections.

Two-group assembly discontinuity factors

As the homogenization was conducted in an infinite lattice model, the ADFs were calculated according to Eq. 43. Here the response is the ratio of a surface detector and a volumetric detector.

Based on symmetry conditions the assembly discontinuity factors were calculated for the south and east sides of the assembly. The ADFs for the two sides should be equal in the TMI1-assembly and differ in the PB2 assembly.

We'll first set up surface flux detectors for the southern surface and eastern surface of the geometry using the two-group energy structure:

```
det FLXS               de myGS ds sSOUTH -2
det FLXE               de myGS ds sEAST  -2
```

Here the surfaces `sSOUTH` and `sEAST` are superimposed planes covering the southern and eastern edge of the geometry respectively. We'll use the volumetric flux detector also used in the two-group macroscopic cross section calculation to set up the reaction rate ratios as sensitivity responses:

```
sens resp detratio ADFS   FLXS FLX
sens resp detratio ADFE   FLXE FLX
```

6.2.2 Results

The ADF-values calculated as a ratio of the surface flux and volumetric flux detector values needed to be scaled by the V/S_k term in Eq. 43, i.e. the ratio between geometry volume and surface area.

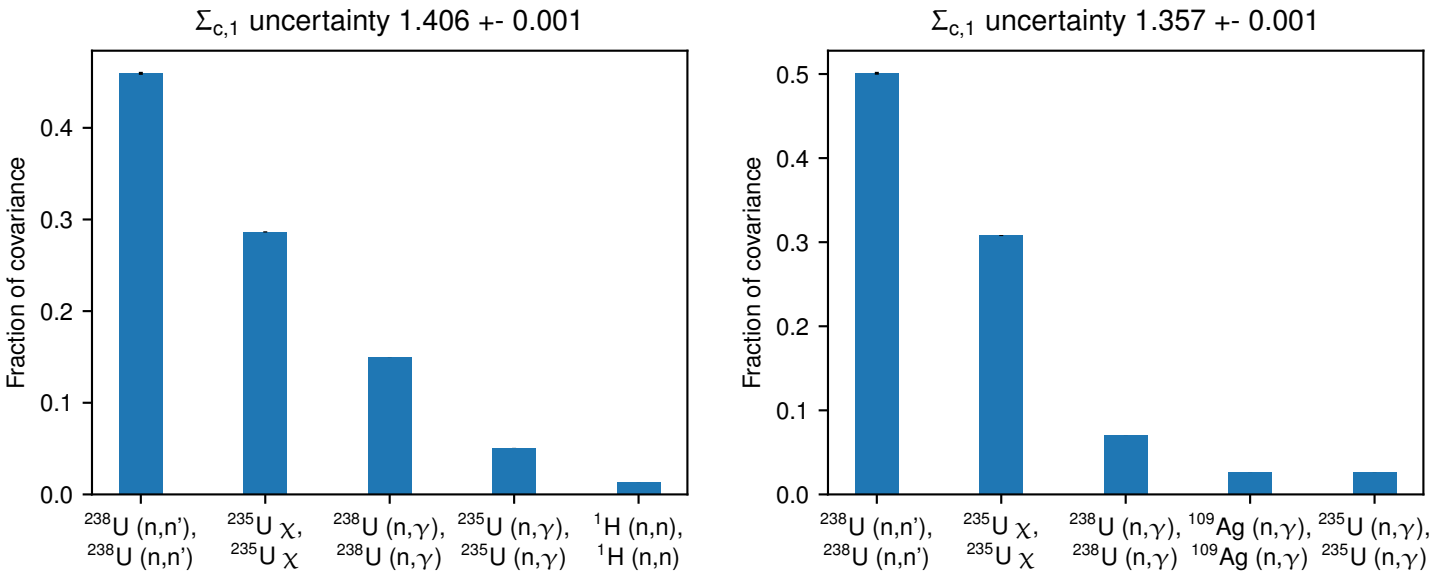

Figure 9. ***TMI1 assembly at HZP:*** *Top contributors (as a fraction of the total covariance) to the uncertainty of the fast capture cross section for the unrodded (**left**) and the rodded (**right**) geometries.*

The results for the unrodded and rodded TMI1 assemblies are shown in Tables 3 and 4. As the values of the group coefficients were calculated from the reaction rates and fluxes in a post-processing step, no information of their statistical uncertainty is available. This is also true for the nuclear data uncertainty of the macroscopic absorption cross section which was calculated from the nuclear data uncertainties of the fission and capture cross sections.

When possible, the results are compared to those calculated by Maria Pusa using CASMO-4E and SCALE-6.0 based covariance data as reported in [14]. It should be noted that as both the transport code and the input covariance data are different between the two results, no good match between the two should be expected. Even so, the calculated values for the group constants are similar between the two methods. The propagated nuclear data uncertainties are larger in the fast group in both the Serpent and the CASMO results with the Serpent propagated uncertainties being typically slightly higher. The larger nuclear data uncertainties in the Serpent results potentially come from the newer covariance data libraries containing additional covariance data (additional known uncertainties) compared to the old libraries.

In future, the results of this uncertainty propagation implementation should be compared to a sampling based method using the same covariance data libraries and Serpent as the transport code.

The largest nuclear data uncertainty is found in the fast capture cross section being approximately 1.41 % in the unrodded case and 1.36 % in the rodded case. The top contributors to this uncertainty are shown in Fig. 9. The largest contributor in both cases is the inelastic scattering cross section of ^{238}U followed by the fission spectrum of ^{235}U and the radiative capture cross section of ^{238}U.

The nuclear data uncertainty of the effective multiplication factor was between 0.5 and 0.6 percent for the two cases. The main contributors for the nuclear data uncertainty in the multiplication factor is shown in Fig. 10.

Table 3. TMI1 HZP unrodded

Parameter	Value	Nuclear data uncertainty (percent) $\pm 2\sigma$ statistical uncertainty	Ref. value [14] (CASMO-4E)	Ref. uncertainty [14] (CASMO-4E)
k_{eff}	1.39501	0.53311 ± 0.00035	1.411	0.4909
$\Sigma_{\text{ela},1}$	0.53798	1.06682 ± 0.00026	N/A	N/A
$\Sigma_{\text{ela},2}$	1.32279	0.20971 ± 0.00023	N/A	N/A
$\Sigma_{\text{c},1}$	0.00702	1.40617 ± 0.00141	N/A	N/A
$\Sigma_{\text{c},2}$	0.03265	0.80304 ± 0.00010	N/A	N/A
$\Sigma_{\text{a},1}$	0.01062	1.06468 ± 0.00000	0.01029	0.7487
$\Sigma_{\text{a},2}$	0.11100	0.46259 ± 0.00000	0.1084	0.2164
$\Sigma_{\text{f},1}$	0.00360	0.39799 ± 0.00040	N/A	N/A
$\Sigma_{\text{f},2}$	0.07835	0.32073 ± 0.00012	N/A	N/A
$(\nu\Sigma_{\text{f}})_1$	0.00908	0.73784 ± 0.00036	0.00885	0.5152
$(\nu\Sigma_{\text{f}})_2$	0.19092	0.50139 ± 0.00008	0.1878	0.4447
$\text{ADF}_{\text{S},1}$	0.97704	0.27540 ± 0.00358	N/A	N/A
$\text{ADF}_{\text{S},2}$	1.04002	0.66647 ± 0.01133	N/A	N/A
$\text{ADF}_{\text{E},1}$	0.97702	0.27188 ± 0.00353	N/A	N/A
$\text{ADF}_{\text{E},2}$	1.04013	0.65505 ± 0.00983	N/A	N/A

Table 4. TMI1 HZP rodded

Parameter	Value	Nuclear data uncertainty (percent) $\pm 2\sigma$ statistical uncertainty	Ref. value [14] (CASMO-4E)	Ref. uncertainty [14] (CASMO-4E)
k_{eff}	1.05810	0.58728 ± 0.00065	1.083	0.5038
$\Sigma_{\text{ela},1}$	0.52472	1.05153 ± 0.00025	N/A	N/A
$\Sigma_{\text{ela},2}$	1.26387	0.22369 ± 0.00025	N/A	N/A
$\Sigma_{\text{c},1}$	0.00974	1.35667 ± 0.00133	N/A	N/A
$\Sigma_{\text{c},2}$	0.05787	0.48911 ± 0.00038	N/A	N/A
$\Sigma_{\text{a},1}$	0.01321	1.10938 ± 0.00000	0.01275	0.7113
$\Sigma_{\text{a},2}$	0.13781	0.39460 ± 0.00000	0.13280	0.1871
$\Sigma_{\text{f},1}$	0.00347	0.41624 ± 0.00037	N/A	N/A
$\Sigma_{\text{f},2}$	0.07994	0.32619 ± 0.00016	N/A	N/A
$(\nu\Sigma_{\text{f}})_1$	0.00878	0.76224 ± 0.00037	0.00857	0.5251
$(\nu\Sigma_{\text{f}})_2$	0.19478	0.50488 ± 0.00010	0.1909	0.4461
$\text{ADF}_{\text{S},1}$	1.01618	0.32875 ± 0.00394	N/A	N/A
$\text{ADF}_{\text{S},2}$	1.37894	0.81794 ± 0.01227	N/A	N/A
$\text{ADF}_{\text{E},1}$	1.01644	0.31864 ± 0.00414	N/A	N/A
$\text{ADF}_{\text{E},2}$	1.37877	0.79338 ± 0.01111	N/A	N/A

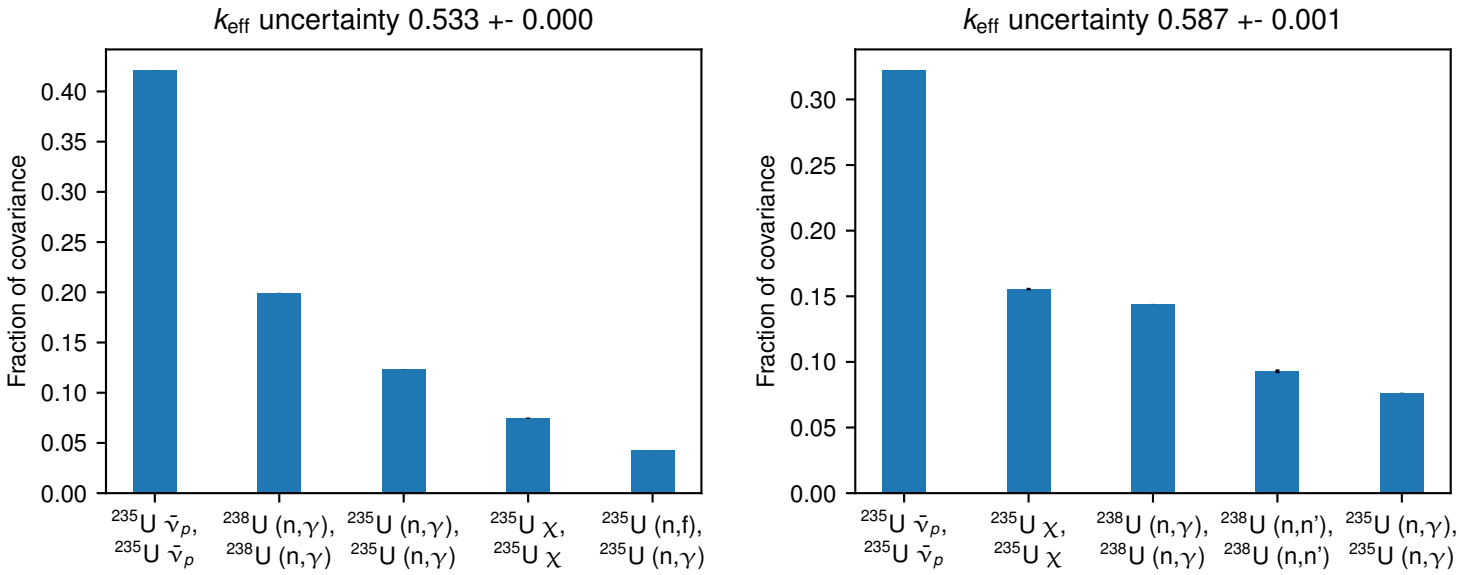

Figure 10. ***TMI1 assembly at HZP:*** *Top contributors (as a fraction of the total covariance) to the uncertainty of the effective multiplication factor for the unrodded (**left**) and the rodded (**right**) geometries.*

Similar analyses can be conducted for all of the different simulated cases and result variables but without relevant reference data or application, such analyses are of limited interest. The other results for the assembly cases are included in the appendices.

7. Limitations and future work

As noted previously, the derivations and implementations hold only for sensitivities of non-leakage-corrected group constants. In order to estimate the uncertainties of leakage corrected group constants a separate methodology needs to be derived for propagating the infinite spectrum multi-group uncertainties through the leakage correction.

This methodology cannot be easily used for propagating the uncertainties through a burnup calculation. While it is possible (although computationally demanding) to calculate the uncertainties in the different transmutation cross sections and depletion fluxes used in forming the Bateman equations, propagating the uncertainties to the solution of the Bateman equations would require a significant amount of additional work and derivation and might not be very feasible.

The calculation of several sensitivities was not implemented in this work as they could be only calculated as sensitivities of detector ratios, for which the required detector response is not available yet. The actual calculation of these group constants is achieved without the use of detectors, i.e. the reaction rates are scored separately outside the detector scoring routines, e.g. in `scorepoison.c` and `scoregc.c`. The calculation of the sensitivities requires either adding the required detector responses and calculating the sensitivities using the automatic detector ratio sensitivity calculation routines or calculating the sensitivities separately, e.g. in `scorepoison.c` and `scoregc.c`. The missing group constants and required detector responses are listed in the following:

- Sensitivity of the *absorption cross section* requires a detector response for tallying the **absorption reaction rate**. Currently the sensitivity can be calculated from the sensitivities of fission and capture cross sections in post-batch processing.
- Sensitivity of the *slowing down cross section* requires a detector response for tallying the **slowing down reaction rate**.
- Sensitivity of the *fission poison production cross section* requires a detector response for tallying the **fission poison production rate**.
- Sensitivity of the *out-scatter diffusion coefficient* requires a detector response for tallying the **P1 scattering cross section**.

The automatic set up of the correct sensitivity calculation responses when group constants are being generated is also left to a future time. At the same point of time it would be possible to implement routines for the automatic direct and inverse energy group condensation of the sensitivities, which would also need the automatic set up of the multi-group and few-group structures that would be used for the sensitivity calculation.

A future optimization would be to use eigendecomposition of the covariance matrices to score the uncertainty contributions from each energy group and reaction mode during neutron transport in effect applying the Sandwich rule (Eq. 8) during neutron transport. This would eliminate the need to calculate and store the sensitivity vectors, which can save computation time and will certainly save memory. See [15] for a continuous energy example of this.

8. Summary

The Serpent Monte Carlo code was extended to read in multi-group nuclear covariance data and use it with previously implemented sensitivity calculation capabilities to propagate nuclear data uncertainties into several different group constants that can be expressed as reaction rate or detector tally value ratios. The uncertainty propagation can also be conducted for the delayed neutron parameters β_{eff} and λ as well as the prompt neutron lifetime ℓ_{eff}.

Several other extensions were also implemented that pave the road for implementing automated uncertainty propagation for generated group and time constants. These include automatically calculating the direct term of the reaction rate sensitivity, adding support for automatic treatment of multi-bin reaction rate ratios as sensitivity responses and including the calculation of sensitivities for the group-wise delayed neutron fractions and delayed neutron precursor decay constants.

As several group constants could not be calculated using the available detector response functions, the theoretical work required for calculating the sensitivities was conducted and listed. In the future, the required detector response functions may either be added or a separate treatment can be implemented to calculate these sensitivities separately from the automatic reaction rate ratio sensitivities.

The capabilities were demonstrated in calculations where detectors were set up to tally reaction rates and fluxes and the group constants were calculated as a post processing step. This approach was used to make use of the previously implemented capability of calculating sensitivities of detector tally value ratios. In the future, the process can be implemented into the routines responsible specifically for group constant generation, where no detectors are used.

Comparisons of several calculated uncertainty values against previous results obtained with CASMO-4E using an older covariance library were promising, but the differences in the exact values are noticeable as can be expected due to the different transport solver and covariance data utilized.

In the future, a sampling based method should be used to verify the propagated nuclear data uncertainties.

References

[1] J. Leppänen et al. "The Serpent Monte Carlo code: Status, development and applications in 2013". *Annals of Nuclear Energy* 82 (2015), pp. 142–150. ISSN: 0306-4549. DOI: 10.1016/j.anucene.2014.08.024. http://www.sciencedirect.com/science/article/pii/S0306454914004095.

[2] J. Leppänen, R. Mattila, and M. Pusa. "Validation of the Serpent–ARES code sequence using the MIT BEAVRS benchmark – Initial core at HZP conditions". *Annals of Nuclear Energy* 69 (2014), pp. 212–225. DOI: 10.1016/j.anucene.2014.02.014. http://www.sciencedirect.com/science/article/pii/S030645491400084X.

[3] J. Leppänen and R. Mattila. "Validation of the Serpent–ARES code sequence using the MIT BEAVRS benchmark – HFP conditions and fuel cycle 1 simulations". *Annals of Nuclear Energy* 96 (2016), pp. 324–331. DOI: 10.1016/j.anucene.2016.06.014. http://www.sciencedirect.com/science/article/pii/S0306454916304121.

[4] J. Kuopanportti, S. Saarinen, and J. Leppänen. "Assessment of Serpent cross sections of the second generation fuel of TVEL for Loviisa NPP". In: *Proc. PHYSOR 2018*. Cancun, Mexico, Apr. 2018.

[5] V. Valtavirta, M. Aufiero, and J. Leppänen. "Collision-history based sensitivity/perturbation calculation capabilities in Serpent 2.1.30". In: *Proc. BEPU 2018*. Lucca, Italy, May 2018.

[6] M. Aufiero et al. "A collision history-based approach to sensitivity/perturbation calculations in the continuous energy Monte Carlo code SERPENT". *Annals of Nuclear Energy* 85 (2015), pp. 245–258. DOI: 10.1016/j.anucene.2015.05.008. http://www.sciencedirect.com/science/article/pii/S0306454915002650.

[7] J. Leppänen, M. Pusa, and E. Fridman. "Overview of methodology for spatial homogenization in the Serpent 2 Monte Carlo code". *Annals of Nuclear Energy* 96 (2016), pp. 126–136. DOI: 10.1016/j.anucene.2016.06.007. http://www.sciencedirect.com/science/article/pii/S0306454916303899.

[8] B. T. Rearden and M. A. Jessee. *SCALE code system*. Version 6.2.1. ORNL/TM-2005/39. 2016. Chap. 6.5.A.5 COVERX format.

[9] R. E. MacFarlane et al. *The NJOY Nuclear Data Processing System, Version 2016*. Version NJOY2016.35. LA-UR-17-20093. 2018. Chap. 11.

[10] R. Vanhanen. *Quality Assurance Methods for Uncertainty Analysis in Reactor Physics with Applications*. PhD thesis. School of Science, Aalto University, 2016. http://urn.fi/URN:ISBN:978-952-60-6730-8.

[11] D. Rochmann and A. Koning. "How to Randomly Evaluate Nuclear Data: A New Data Adjustment Method Applied to 239Pu". *Nuclear Science and Engineering* 169.1 (2011), pp. 68–80. DOI: 10.13182/NSE10-66. eprint: https://doi.org/10.13182/NSE10-66. https://doi.org/10.13182/NSE10-66.

[12] I. A. Kodeli, M. Aufiero, and W. Zwermann. "Comparison of deterministic and Monte Carlo codes SUS3D, Serpent and XSUSA for beta-effective sensitivity calculations". In: *Proc. PHYSOR 2016*. Sun Valley, ID, USA, May 2016.

[13] K. Ivanov et al. *Benchmark for Uncertainty Analysis in Modelling (UAM) for the Design, Operation and Safety Analysis of LWRs, Volume I: Specification and Support Data for Neutronics Cases (Phase I)*. OECD/NEA. 2013.

[14] M. Pusa. "Adjoint-based Uncertainty Analysis of Lattice Physics Calculations". In: *Proc. Physor 2014*. Kyoto, Japan, 28 Sep. – 3rd Oct 2014.

[15] M. Aufiero, M. Martin, and M. Fratoni. "XGPT: Extending Monte Carlo Generalized Perturbation Theory capabilities to continuous-energy sensitivity functions". *Annals of Nuclear Energy* 96 (2016), pp. 295–306. DOI: 10.1016/j.anucene.2016.06.012. http://www.sciencedirect.com/science/article/pii/S0306454916302572.

Appendices

A Pin cell HZP results

Table A.1. PB2 pin-cell HZP

Parameter	Value	Nuclear data uncertainty (percent) $\pm 2\sigma$ statistical uncertainty
k_{eff}	1.30547	0.60301 $\pm$ 0.00145
$\sigma_{\text{c,5}}$	1.13300	1.73072 $\pm$ 0.00260
$\sigma_{\text{c,8}}$	0.08809	1.46947 $\pm$ 0.00367
$\sigma_{\text{a,5}}$	6.33737	1.31072 $\pm$ 0.00000
$\sigma_{\text{a,8}}$	0.09832	1.84291 $\pm$ 0.00000
$\sigma_{\text{f,5}}$	5.20437	1.21928 $\pm$ 0.00378
$\sigma_{\text{f,8}}$	0.01023	5.05866 $\pm$ 0.00556
Σ_c	0.01035	1.22853 $\pm$ 0.00270
Σ_a	0.02201	1.04052 $\pm$ 0.00000
Σ_f	0.01166	0.87367 $\pm$ 0.00341

Table A.2. TMI1 pin-cell HZP

Parameter	Value	Nuclear data uncertainty (percent) $\pm 2\sigma$ statistical uncertainty
k_{eff}	1.40630	0.55094 $\pm$ 0.00127
$\sigma_{\text{c,5}}$	0.90231	1.78068 $\pm$ 0.00267
$\sigma_{\text{c,8}}$	0.08971	1.50794 $\pm$ 0.00422
$\sigma_{\text{a,5}}$	4.73510	1.37493 $\pm$ 0.00000
$\sigma_{\text{a,8}}$	0.10104	1.88909 $\pm$ 0.00000
$\sigma_{\text{f,5}}$	3.83279	1.27941 $\pm$ 0.00397
$\sigma_{\text{f,8}}$	0.01133	4.90764 $\pm$ 0.00589
Σ_c	0.01031	1.30080 $\pm$ 0.00325
Σ_a	0.02404	1.11108 $\pm$ 0.00000
Σ_f	0.01373	0.96862 $\pm$ 0.00378

B Peach Bottom 2 assembly HZP results

Table B.1. PB2 assembly HZP unrodded

Parameter	Value	Nuclear data uncertainty (percent) $\pm 2\sigma$ statistical uncertainty
k_{eff}	1.11286	0.59842 ± 0.00066
$\Sigma_{\text{ela},1}$	0.54559	0.99027 ± 0.00035
$\Sigma_{\text{ela},2}$	1.44781	0.17283 ± 0.00026
$\Sigma_{\text{c},1}$	0.00527	1.31028 ± 0.00210
$\Sigma_{\text{c},2}$	0.02666	0.61558 ± 0.00025
$\Sigma_{\text{a},1}$	0.00721	1.20773 ± 0.00000
$\Sigma_{\text{a},2}$	0.05520	0.47000 ± 0.00000
$\Sigma_{\text{f},1}$	0.00194	0.92914 ± 0.00121
$\Sigma_{\text{f},2}$	0.02854	0.33404 ± 0.00028
$(\nu\Sigma_{\text{f}})_1$	0.00499	1.41842 ± 0.00104
$(\nu\Sigma_{\text{f}})_2$	0.06955	0.50990 ± 0.00019
$\text{ADF}_{\text{S},1}$	0.88721	0.34919 ± 0.00489
$\text{ADF}_{\text{S},2}$	1.77478	0.34909 ± 0.00559
$\text{ADF}_{\text{E},1}$	0.95615	0.23841 ± 0.00715
$\text{ADF}_{\text{E},2}$	1.29269	0.39986 ± 0.00680

Table B.2. PB2 assembly HZP rodded

Parameter	Value	Nuclear data uncertainty (percent) $\pm 2\sigma$ statistical uncertainty
k_{eff}	0.86308	0.59806 ± 0.00072
$\Sigma_{\text{ela},1}$	0.53723	0.98126 ± 0.00029
$\Sigma_{\text{ela},2}$	1.36442	0.18591 ± 0.00024
$\Sigma_{\text{c},1}$	0.00788	1.14615 ± 0.00183
$\Sigma_{\text{c},2}$	0.04237	0.45495 ± 0.00045
$\Sigma_{\text{a},1}$	0.00981	1.09716 ± 0.00000
$\Sigma_{\text{a},2}$	0.07517	0.40288 ± 0.00000
$\Sigma_{\text{f},1}$	0.00193	0.89704 ± 0.00090
$\Sigma_{\text{f},2}$	0.03280	0.33561 ± 0.00023
$(\nu\Sigma_{\text{f}})_1$	0.00496	1.38504 ± 0.00080
$(\nu\Sigma_{\text{f}})_2$	0.07992	0.51105 ± 0.00015
$\text{ADF}_{\text{S},1}$	0.74092	0.78946 ± 0.00568
$\text{ADF}_{\text{S},2}$	0.49143	0.74350 ± 0.01264
$\text{ADF}_{\text{E},1}$	1.05622	0.28033 ± 0.00308
$\text{ADF}_{\text{E},2}$	1.98379	0.39268 ± 0.00432

C Peach Bottom 2 assembly HFP results

Table C.1. PB2 assembly HFP unrodded

Parameter	Value	Nuclear data uncertainty (percent) $\pm 2\sigma$ statistical uncertainty
k_{eff}	1.06978	0.66871 ± 0.00087
$\Sigma_{\text{ela},1}$	0.39079	1.04209 ± 0.00031
$\Sigma_{\text{ela},2}$	0.89930	0.22523 ± 0.00021
$\Sigma_{\text{c},1}$	0.00511	1.39744 ± 0.00182
$\Sigma_{\text{c},2}$	0.02438	0.62338 ± 0.00031
$\Sigma_{\text{a},1}$	0.00692	1.27818 ± 0.00000
$\Sigma_{\text{a},2}$	0.05239	0.47045 ± 0.00000
$\Sigma_{\text{f},1}$	0.00181	0.94153 ± 0.00104
$\Sigma_{\text{f},2}$	0.02801	0.33736 ± 0.00023
$(\nu\Sigma_{\text{f}})_1$	0.00464	1.39384 ± 0.00091
$(\nu\Sigma_{\text{f}})_2$	0.06826	0.51213 ± 0.00015
$\text{ADF}_{\text{S},1}$	0.93725	0.25592 ± 0.00486
$\text{ADF}_{\text{S},2}$	1.67003	0.38280 ± 0.00612
$\text{ADF}_{\text{E},1}$	0.97447	0.20141 ± 0.00342
$\text{ADF}_{\text{E},2}$	1.20622	0.44337 ± 0.01286

Table C.2. PB2 assembly HFP rodded

Parameter	Value	Nuclear data uncertainty (percent) $\pm 2\sigma$ statistical uncertainty
k_{eff}	0.76654	0.75575 ± 0.00121
$\Sigma_{\text{ela},1}$	0.39026	1.02301 ± 0.00028
$\Sigma_{\text{ela},2}$	0.85482	0.24475 ± 0.00022
$\Sigma_{\text{c},1}$	0.00760	1.27706 ± 0.00153
$\Sigma_{\text{c},2}$	0.04126	0.44842 ± 0.00054
$\Sigma_{\text{a},1}$	0.00937	1.21495 ± 0.00000
$\Sigma_{\text{a},2}$	0.07256	0.40211 ± 0.00000
$\Sigma_{\text{f},1}$	0.00176	0.94696 ± 0.00091
$\Sigma_{\text{f},2}$	0.03130	0.34106 ± 0.00028
$(\nu\Sigma_{\text{f}})_1$	0.00452	1.40023 ± 0.00080
$(\nu\Sigma_{\text{f}})_2$	0.07628	0.51466 ± 0.00019
$\text{ADF}_{\text{S},1}$	0.80977	0.58728 ± 0.00411
$\text{ADF}_{\text{S},2}$	0.47754	0.83391 ± 0.01251
$\text{ADF}_{\text{E},1}$	1.04964	0.25661 ± 0.00282
$\text{ADF}_{\text{E},2}$	1.85195	0.47870 ± 0.00622

D Three Mile Island 1 assembly HFP results

Table D.1. TMI1 assembly HFP unrodded

Parameter	Value	Nuclear data uncertainty (percent) $\pm 2\sigma$ statistical uncertainty
k_{eff}	1.37892	0.53934 ± 0.00036
$\Sigma_{\text{ela},1}$	0.52908	1.07159 ± 0.00028
$\Sigma_{\text{ela},2}$	1.28959	0.21318 ± 0.00023
$\Sigma_{\text{c},1}$	0.00719	1.41224 ± 0.00140
$\Sigma_{\text{c},2}$	0.03221	0.80550 ± 0.00010
$\Sigma_{\text{a},1}$	0.01078	1.07555 ± 0.00000
$\Sigma_{\text{a},2}$	0.10967	0.46384 ± 0.00000
$\Sigma_{\text{f},1}$	0.00358	0.39977 ± 0.00040
$\Sigma_{\text{f},2}$	0.07746	0.32177 ± 0.00012
$(\nu\Sigma_{\text{f}})_1$	0.00905	0.73925 ± 0.00035
$(\nu\Sigma_{\text{f}})_2$	0.18874	0.50206 ± 0.00008
$\text{ADF}_{\text{S},1}$	0.97768	0.27462 ± 0.00384
$\text{ADF}_{\text{S},2}$	1.03774	0.67032 ± 0.00938
$\text{ADF}_{\text{E},1}$	0.97760	0.26980 ± 0.00351
$\text{ADF}_{\text{E},2}$	1.03827	0.67701 ± 0.01151

Table D.2. TMI1 assembly HFP rodded

Parameter	Value	Nuclear data uncertainty (percent) $\pm 2\sigma$ statistical uncertainty
k_{eff}	1.04259	0.60130 ± 0.00427
$\Sigma_{\text{ela},1}$	0.51630	1.05677 ± 0.00180
$\Sigma_{\text{ela},2}$	1.23284	0.22960 ± 0.00158
$\Sigma_{\text{c},1}$	0.00988	1.37125 ± 0.00617
$\Sigma_{\text{c},2}$	0.05754	0.48665 ± 0.00433
$\Sigma_{\text{a},1}$	0.01334	1.12260 ± 0.00000
$\Sigma_{\text{a},2}$	0.13653	0.39392 ± 0.00000
$\Sigma_{\text{f},1}$	0.00346	0.41264 ± 0.00227
$\Sigma_{\text{f},2}$	0.07899	0.32637 ± 0.00101
$(\nu\Sigma_{\text{f}})_1$	0.00875	0.75746 ± 0.00265
$(\nu\Sigma_{\text{f}})_2$	0.19248	0.50513 ± 0.00066
$\text{ADF}_{\text{S},1}$	1.01684	0.38258 ± 0.07652
$\text{ADF}_{\text{S},2}$	1.37552	0.86463 ± 0.07609
$\text{ADF}_{\text{E},1}$	1.01564	0.30500 ± 0.02623
$\text{ADF}_{\text{E},2}$	1.37345	0.79002 ± 0.04898